# Development of a Load Inductor in a Single Pulse Test Circuit

*Master of Science Thesis*

*HOSSEIN EMAMJOMEH*

Department of Energy and Environment

Division of Electric Power Engineering

CHALMERS UNIVERSITY OF TECHNOLOGY

Gothenburg, Sweden 2013

Development of a Load Inductor in a Single Pulse Test Circuit

*HOSSEIN EMAMJOMEH*



*hossein_emamjomeh@yahoo.com*

*Department of Energy and Environment*

*Division of Electric Power Engineering*

*Chalmers University of Technology*

*SE–412 96 Göteborg,*

*Sweden*

*Telephone +46 (0)31–772 1000*

*Chalmers Bibliotek, Reproservice*

*Göteborg, Sweden 2013*

*To my lovely girlfriend, Maryam*

*And*

*My parents for their endless love, support and encouragement…*

Development of a Load Inductor in a Single Pulse Test Circuit

*HOSSEIN EMAMJOMEH*

*Department of Energy and Environment*

*Division of Electric Power Engineering*

*Chalmers University of Technology*

## Abstract

In this work, with the purpose of reducing the surrounding disturbance field, a toroidal inductor for a single pulse test circuit is designed and a prototype is manufactured. The manufactured toroidal inductor is 355µH while the existing cylindrical inductor is 270µH.

In addition, the designed inductor together with the existing cylindrical inductor of the single pulse test circuit are implemented in the COMSOL Multiphysics® program in order to make a comparison of the magnetic field and to investigate the disturbance of both type of the inductors on the test results of the single pulse test circuit. According to the test results and the comparison made in COMSOL Multiphysics®, it is observed that the magnetic field of the toroidal inductor is much less than the one of the cylindrical inductor for the same current (1.8kA) and inductance value (270µH). The magnetic field of the toroidal inductor shows a dramatic reduction compared to the magnetic field of the cylindrical inductor. At a horizontal distance of 10cm from the inductors, the magnetic field is reduced from 42.798µT in the cylindrical inductor case to 2.423µT in the toroidal inductor case; likewise at a vertical distance of 10cm from the inductors, the magnetic field is reduced from 15.999µT in the cylindrical inductor case to 0.850µT in the toroidal inductor case.

Furthermore, 40A is applied to the inductors in order to measure and compare the magnetic field of the existing 270µH cylindrical inductor and 355µH manufactured toroidal inductor. The measurement shows that at a distance of 10cm, the magnetic flux density is reduced from 307µT in the cylindrical inductor case to 0.28µT in the toroidal

inductor case; however the inductor value of the toroidal inductor is higher than cylindrical inductor (355μH compared to 270μH).

Moving the circular loop 10cm away from the cylindrical inductor, the magnetic field reduces by 43%, likewise when the distance increases to 20cm, the magnetic field reduction is 61%.

In this thesis a significant reduction of magnetic field in the toroidal inductor compared with cylindrical inductor is achieved. At the moment of writing this report, so far, the highest current level and voltage level applied to the manufactured toroidal inductor are 2000A and 3600V, respectively.

Key words: Cylindrical Inductor, Magnetic field, Semiconductor, Single pulse test, Toroidal Inductor

## Acknowledgements

This master thesis has been written for Chalmers University of Technology, Gothenburg, Sweden, and ABB, Ludvika, Sweden which is the end of my master program and the restart of my professional carrier. For the last 8 months, I have been part of ABB's development team; working besides the experts and getting in practice their experiences were a precious opportunity for me. I would like to express my sincere gratitude to Poopak Roshanfekr Fard and my examiner Professor Torbjörn Thiringer for their patience, support and help to find such a genuine master thesis and to thank R & D department at ABB Ludvika, Arman Hassanpoor, Jurgen Hafner, and Bjorn Jacobson for their trust and giving me this opportunity to undertake the thesis. I would like to express my "most" sincere appreciation to my supervisor Mika Seppänen for sharing his untouched experiences, cooperation, continuous support and inspiration with the enhancement of my work. Yuriy Serdyuk is also greatly appreciated for the support and help in the COMSOL Multiphysics® simulation and offering critical comments. Many helpful comments were provided by my colleagues at valve testing department which are greatly appreciated. ABB has sponsored my work and accommodation in Ludvika which is gratefully acknowledged. Last but not least, I would like to thank ABBs HVDC Light project team and wish good luck with the future development!

*Hossein Emamjomeh*

*Ludvika, Sweden, 2013*

# Contents

# 1 Introduction

A growing large variety of high power semiconductors with high reliability are being applied in traction, industry applications and energy transmission technology. At the moment ABB, a leader in power and automation technologies, designs and manufactures high power semiconductors in the power range of 300 up to 12000A and 200 up to 8500V. These products are used in many technologies such as High Voltage Direct Current (HVDC) transmission systems, traction systems, and renewable energy generation [1].

## 1.1 Problem background

Power semiconductor devices are greatly applied in HVDC electric power transmission system. A number of series connected semiconductor devices is technically called semiconductor valve which is the heart of the HVDC system required for the conversion from alternating current(AC) to direct current(DC) or vice versa[1].

Power electronic switching devices in power electronics system seem to behave differently confronting different operating position; therefore, their behavior needs to be carefully studied before applying the device in the technology. All semiconductors are needed to be tested dynamically and statically at different operating temperatures prior to shipment. These tests encompass the standardized production control tests and the final test [1]. The final test is made to confirm if the manufactured product is in accordance with the customer specifications and also to check the proper operation of the system and the valve functionality. This kind of tests are called “routine test”. There is also another kind of test called “development test” which is performed in order to develop and to enhance the devices. One of the development tests is the single pulse test (SPT) which is executed to investigate the behavior of the switch in a semi-actual operating point. Since the investigation and the development of the device are made according to the single pulse test, the results, waveforms and the data acquired from the test are important, and accordingly need to be exact and precise. In order to obtain a clear and unambiguous result, the components of the test circuit are supposed to be standardized and the undesired circuit component disturbances on the result need to be eliminated.

## 1.2 Previous work

To investigate the behavior of semiconductor devices, a single pulse test (SPT) is commonly applied. According to the test object and the test circuit components, the pulses are sent to the device with a specific time sequence, switching the device in order to open or to close the circuit for particular current amplitude. Eventually, the semiconductor behavior is analyzed and investigated. In the test circuit (which will be explained later on), there is a cylindrical inductor called "load inductor" applied in order to control the current rise rate. This inductor also provides disturbances on the test results due to the magnetic field spreading. In order to reduce the inductor magnetic field spreading out and the disturbances on the test results, a shield has to be placed on the inductor or the inductor has to be located far from the other circuit component and the measuring devices.

## 1.3 Purpose

The main purpose of this thesis is to accomplish the following tasks:

- Investigate the single pulse test circuit and the inductor role in the circuit
- Design a toroidal load inductor for the single pulse test circuit in order to reduce the magnetic field disturbance
- The designed inductor and the existing inductor implementation in COMSOL Multiphysics®
- Manufacturing a prototype of the designed inductor
- Magnetic field measurement of the existing inductor as well as the designed inductor, in order to verify the magnetic field reduction
- Execute a single pulse test with the new inductor

# 2 Single Pulse Test circuit

In order to study the behavior of the semiconductor devices in the circuit, a single pulse test (SPT) can be used. Fig. 2.1 illustrates such a single pulse test circuit.

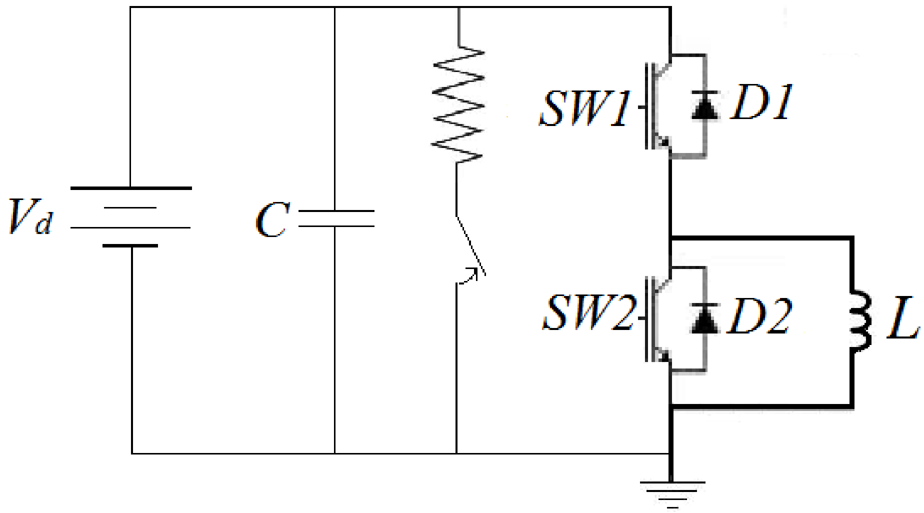


**Fig. 2.1 Simplified single-pulse test circuit**

The supply unit generates voltage which charges the capacitor. The pulse generator sends the pulses in order to trigger the gate unit according to the calculated time sequences. The test object is switched on and off and the charged capacitor is being discharged while the current passes through the test object. There are two IGBTs used in the single pulse test circuit Fig. 2.1.The upper IGBT is the test object while the lower IGBT is always switched off, which means, only the anti paralleled diode plays the role. The current flows through the test object according to the calculated time sequences. The behavior of the test object (upper IGBT) is investigated and the losses are estimated. Finally, in order to fully discharge the capacitor after the test, the resistor will be connected to the circuit, and the charges in the capacitor are discharged through this bleed resistor. In this circuit, an inductor is required in order to govern the current rising rate. All components of this circuit will be explained briefly in the next sub-chapter.

## 2.1 Circuit components

An investigation of the SPT circuit components seems to be helpful in the comprehension of the testing procedure and in the design of the load inductor. In this subchapter, initially, the semiconductor devices, which are the main components in this test circuit, are described. Afterward, the other components of the circuit such as capacitor and bleed resistor are shortly presented. Finally, the load inductor is introduced and the role of this component is presented.

### 2.1.1 Semiconductors

If there are mobile charge-carriers free to move, confront an electric field, there would be a current flow in the material. Both free electrons and holes carry the current in the material. There is a wide range in the number of free-carriers in various materials. In conductors like copper or silver, the free-electron density is on the order of $10^{23}cm^{-3}$; while in insulators such as quartz or aluminum oxide the free-electron density is less than $10^{3}cm^{-3}$[2].

Semiconductor materials such as Silicon or gallium arsenide have the free-carrier density between that of the conductors and insulators and it varies from $10^{8}cm^{-3}$ to $10^{19}cm^{-3}$. The free-carrier density in semiconductors can be changed to a significant degree by changing the impurity atoms called “doping” and this capability gives to the semiconductors the most crucial role in power electronics.

Modifications applied to the simple low power devices resulted in high power application devices. Various power electronic devices are manufactured using semiconductor materials and benefit from the semiconductor properties. An ideal power semiconductor device needs to have a large breakdown voltage, low on-state voltage drop and resistance, fast switching transient and a large power dissipation capability[2]. Despite the considerable progress in power electronic devices, there is still no available device which “simultaneously” has the afore-mentioned properties. Accordingly, taking into account the application of the device and its role in the circuit, the ideal properties need to be compromised and different devices with different characteristics are produced.

The thyristor, GTO, IGBT, IGCT and BIGT are the semiconductor devices which are needed to be investigated in the single pulse test in order to study the behavior of the switch in the actual operating situation.

*IGBT*

An insulated gate bipolar transistor (IGBT) is a power semiconductor device with three terminals used as an electronic switch with high efficiency and fast switching performance. Fig. 2.2 shows the circuit symbol and *i-v* characteristics of an IGBT[2].

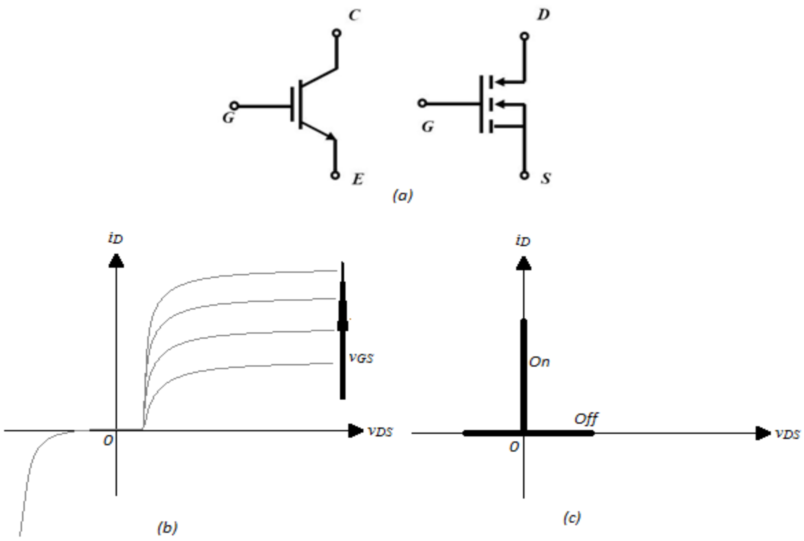


**Fig. 2.2 (a) An IGB symbol; (b) *i-v* characteristics; (c) idealized characteristics**

The IGBT encompasses the advantages of a high impedance gate such as for a MOSFET (hence requires a small energy to switch the gate), high-current and low–saturation-voltage capability (low on-state conduction losses) of a BJT, and like a GTO, it has the ability to block negative voltages. By changing the IGBT gate source voltage, it is also possible to control the turn-on speed of the device [2]. The industry enhancement of IGBTs is growing so fast and these devices are developing at a rapid pace. Nowadays it is possible to find an IGBT which can support 50kA at 10kV[1].

[1] DTI's switch array is a compact assembly of discrete, lower voltage solid-state devices. The switch is made up of five plates, each of which contains 100 lower voltage devices, switched by a common gate drive. Each plate operates at 10 kA, 10 kV; five plates operating in parallel achieve 50 kA at 10 kV for total power of 500 MW. (ref: http://www.divtecs.com/research/high-current-high-voltage-igbt-switch/)

In the test circuit several IGBTs and the anti paralleled diodes are press packed in an IGBT module which is called “StakPak™”. A StakPak™ is made by multiple parallel chips and diodes [1]. Fig. 2.3 shows an IGBT StakPak™ with collector side up and an open sub-module emitter side up.

**Fig. 2.3 ABB StakPak™ module(Courtesy ABB)**

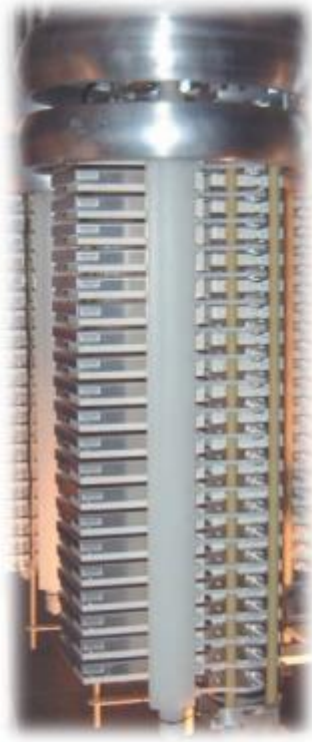

**Fig. 2.4 Standard IGBT valve(Courtesy ABB)**

Several series StakPak™s produce a valve module which is shown in Fig. 2.4. There are two IGBT StakPak™s in the SPT circuit while the lower one is always switched off and only the anti-paralleled diode is used in the test circuit. A driver is connected to the gate unit to ensure that the lower IGBT is always kept off and activated. The upper IGBT is the test object and the pulses are sent to the gate unit to trigger this IGBT’s gate.

### 2.1.2 Gate drive unit and switching

In order to control the switching sequences, the gate drive unit (GU) is introduced. The GU is connected to the gate leg of an IGBT and it controls the current through the switch by triggering the gate. Due to the fact that the power dissipation is too large during traversing the active region, a suitable gate unit is the one that can switch the device quickly to reduce the turn off and turn on times, consequently, to minimize the switching losses[2].

Since real switches are not ideal and they don’t have ideal characteristics, the current through the switch and the voltage over the switch are not zero simultaneously at the switching transition. Fig. 2.5 shows a switch connected to a simple circuit which models a rather common situation in practical application of the switches.

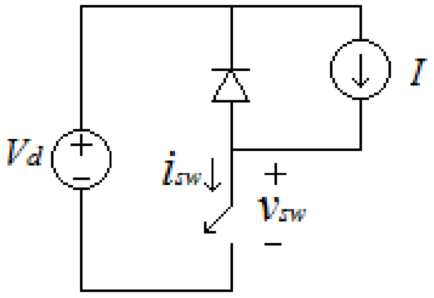


**Fig. 2.5 Simple model of a switching circuit**

In this circuit the current source presents the inductor and since the switch behavior is the point of our interest, the diode is assumed ideal. When the control signal commands the switch to turn it on, the current will start to flow through the switch and the diode is reverse biased. Turning off the switch, the diode takes over the current, and voltage drop over the switch will be equal to the input voltage. In order to visualize, the linearized waveforms are plotted in Fig. 2.6.

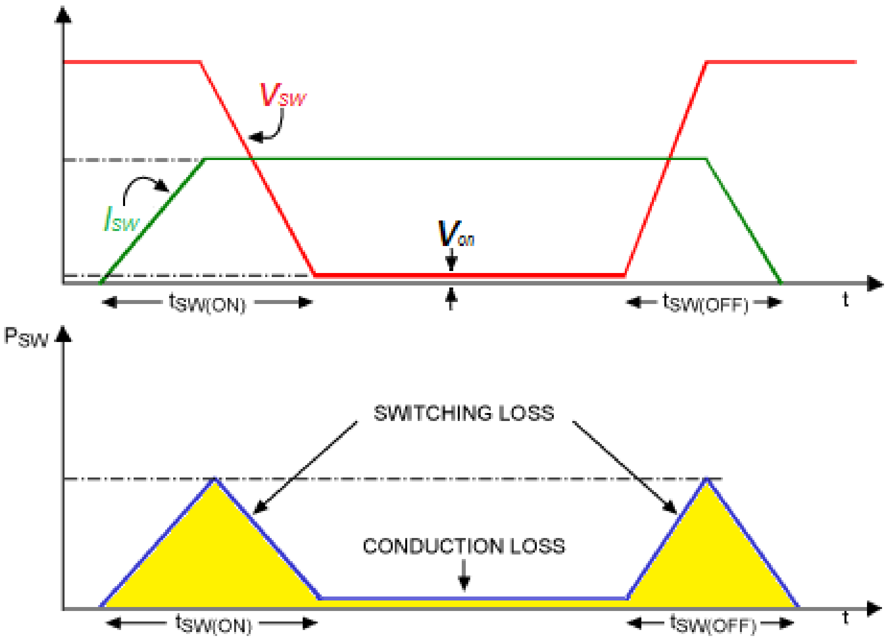


**Fig. 2.6 Linearized switching waveform and the power losses**

When the turn on command is sent, the current starts to flow through the switch and when it reaches the maximum value, the voltage over the switch reduces to on-state voltage. Sending turn of command, the voltage starts to increase to the input voltage value and when it reaches the maximum value, the current decreases to zero. The nonzero current and the nonzero voltage during switching transition produce switching losses. Although the duration of the switching is very short, the switching losses are considerably large since both high voltage and high current exist during the switching moment. Therefore estimation of the turn on and the turn off transition losses is crucial.

### 2.1.3 Diode

The anti paralleled diode in the circuit acts as a freewheeling diode and it handles the inductive load current at turn off. During the turn off period, the current circulates through the anti paralleled diode and the load inductor.

### 2.1.4 Supply unit, capacitors and Rogowski coil

The supply unit is required to charge the capacitors, providing high voltage low current. DC capacitors are used as energy supplier, charged to the appropriate value and then discharged through the IGBT switch. A Rogowski coil is a toroid of wire, wrapped around the cable to measure the current through it. In the single pulse test circuit, in order to measure the fast-changing high amount of current through the capacitor and the switch, Rogowski coils, which are immune to magnetic interferences, are applied to show the current on the oscilloscope screen.

### 2.1.5 Bleed resistors and the NC contactor

Bleed (discharge) resistors are used in order to softly discharge the dc capacitors. The last step after execution of the test is to discharge the capacitors in the bleed resistors. The capacitors need to be always connected to the resistors to be kept discharged, unless the contactor is commanded and the resistors are disconnected from the circuit in order to execute the test.

### 2.1.6 Load inductor

In order to provide the proper current level and to smooth the current rise rate, a load inductor is required. Since the current in the inductor does not vary instantaneously, the load inductance defines the current rise rate. By changing the load inductance, it is possible to change the current rise rate. The larger the inductor, the current rise would be slower.

### *Existing load inductor in the single pulse test circuit:*

There is a cylindrical inductor in the single pulse test circuit. Fig. 2.7 shows a photo of the actual cylindrical inductor in the circuit and properties are found in Table 1.

**Fig. 2.7 Cylindrical inductor in the single pulse test circuit**

**Table 1 Cylindrical inductor properties**

| ***Property*** | ***Value*** |
|---|---|
| *Inductance* | *270µH* |
| *Height* | *34cm* |
| *Diameter* | *20cm* |
| *Cable cross section* | *10mm²* |
| *Number of turns* | *38turns* |
| *Type of winding* | *Single layer* |
| *Core* | *Air core* |
| *Cylinder material* | *Polypropylene* |

The maximum current passing through the inductor needs to be considered during the design of the inductor. Another factor which needs to be observed is the inductor resistance. The inductor series resistance should be minimized in order to avoid the voltage drop over the inductor.

## 2.2 Procedure of a single pulse testing and the duty of the load inductor

Below, the procedure of the single pulse test is briefly presented.

1) **Time sequence calculation:** In order to achieve the desired current levels, a calculation needs to be performed for estimating the pulse sequences. This calculation is carried out according to the test object characteristics and the circuit components.

2) **Disconnection of the bleeding resistors and the ground cable in order to charge the capacitor:** For safety reasons the bleeding resistors are always connected to the capacitor to keep it discharged. In order to charge the capacitors, first it is needed to disconnect the bleeding resistors from the circuit as well as the ground cable. After disconnection of the capacitors from the bleeding resistors, the supply unit will be set to the proper voltage value, while the current is very low, the capacitor will be charged.

3) **Triggering the Gate Unit:** In this stage, the pulses are defined to be sent to the gate unit of the test object.

4) **Switching process:** Triggering the gate and turning the switch on, current passes through the switch. Then another signal is sent to switch off the device. At this time the current passes (circulates) through the load inductor and the freewheeling diode. Two other consecutive pulses are sent in order to perform another switching based on the calculated time sequences.

5) **Monitoring the current and voltage waveform:** An oscilloscope shows the current and voltage waveforms and acquires the data for the switch investigation.

6) **Connection of the bleeding resistors:** After the test, the bleeding resistors are short circuited to the circuit to fully discharge the capacitors.

7) **Study the result:** According to the waveforms and the test results, the switching losses are calculated. The switching losses are obtained from the product multiplication of the instantaneous current through the switch and the instantaneous voltage over the switch. These transient losses are determined according to waveforms provided on the oscilloscope screen which are mostly dependant on test object characteristics, the chip temperature, the commutation inductor and the switching pattern.

Fig. 2.8 shows a rough SPT circuit. The load inductor is the point of interest in this study.

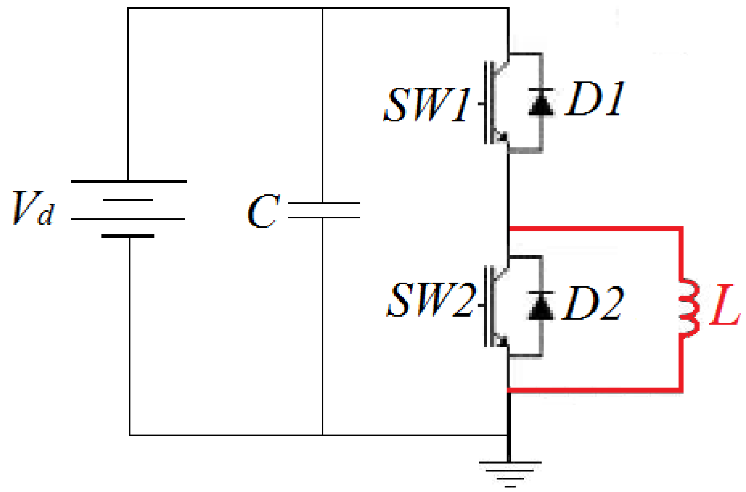


**Fig. 2.8 Rough single pulse test circuit**

It should be always noticed that the test object is SW1 while SW2 is always switched off during the test.

The switching pulses and the voltage and current waveforms are shown in Fig. 2.9.

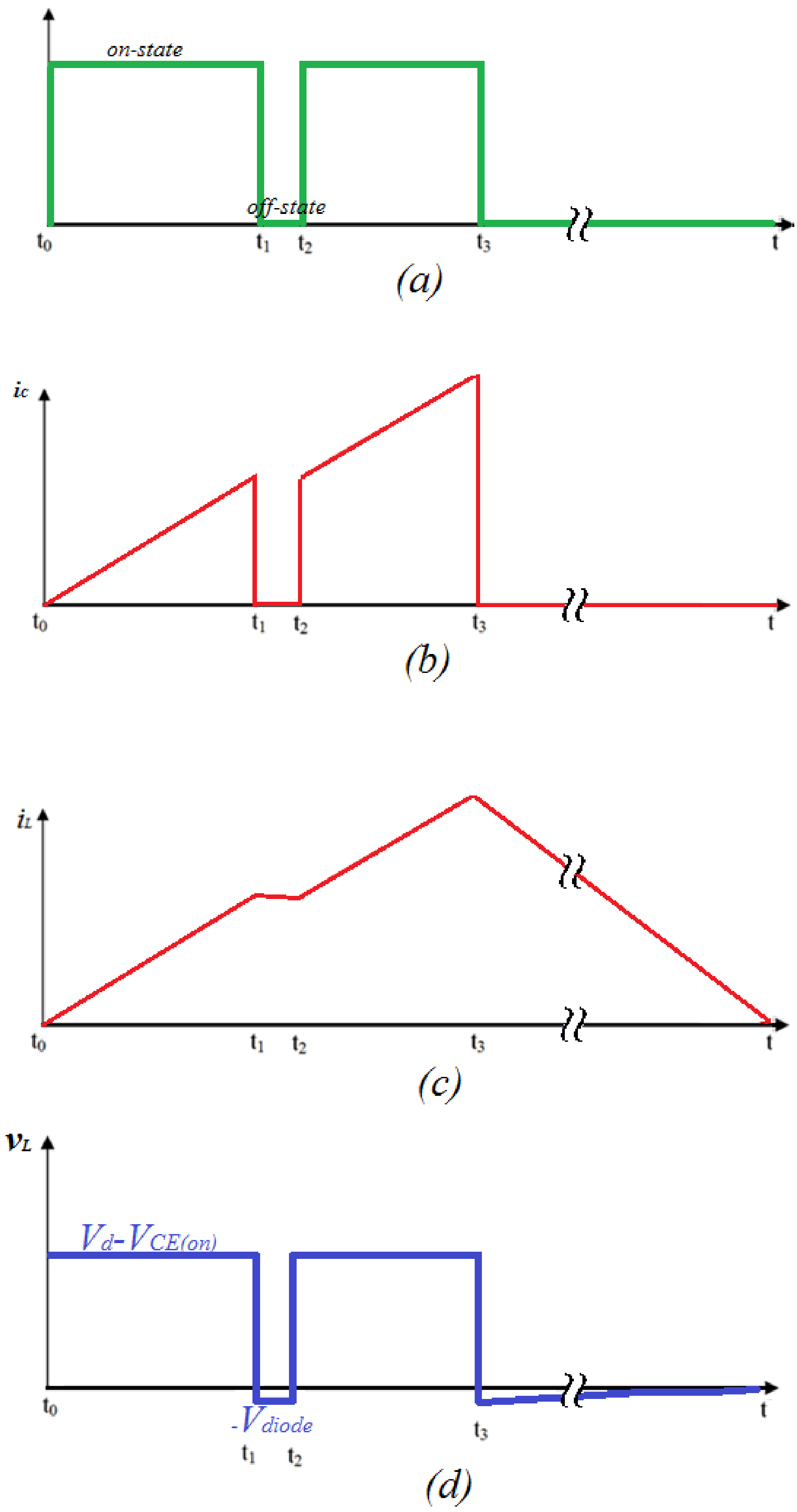


**Fig. 2.9 (a) Switching pulse; (b) Linearized switch current; (c) Load inductor current waveform; (d) Load inductor voltage waveform**

Single pulses are sent to the gate unit in order to switch the test object (see Fig. 2.9 a). The properties of pulses applied to the gate unit are supposed to be in accordance with the design of the gate unit and the specifications which provided by the manufacturer. At $t_0$ the first pulse is sent to the IGBT's gate and the current starts to flow through the switch SW1 and the inductor. Fig. 2.10 shows the current path during switch on-state.

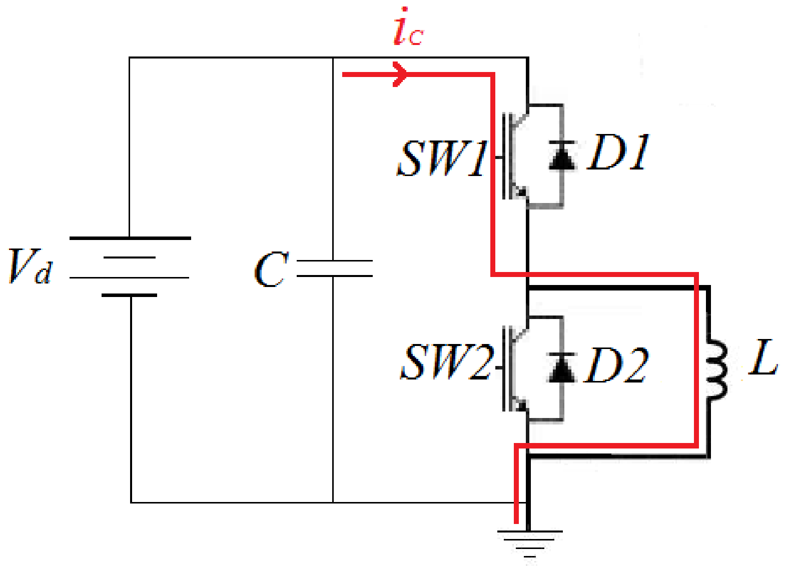


**Fig. 2.10 Current path during the on state**

In this state the collector current starts to rise according to the load inductance value, (see Fig. 2.9a and c)

$$i_c = i_L \tag{2.1}$$

where the inductor current is varying according to the voltage over the inductor,

$$v_L = L\frac{di_L}{dt} \tag{2.2}$$

During on-state, (see Fig. 2.9 d)

$$v_{L(on-state)} = V_d - V_{CE(on)} \cong V_d \tag{2.3}$$

After a specific time, at t1, the second pulse is sent to turn the switch off. Since the sudden current change in the inductor is not possible, the anti-paralleled diode of the lower IGBT takes over the current from the test object. In this state, the current is freewheeling through the inductor and the diode, as it is shown in Fig. 2.11.

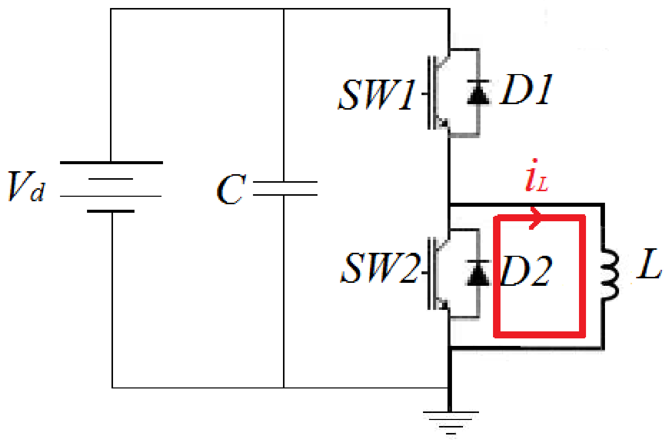


**Fig. 2.11 Freewheeling current through the inductor and the diode**

Consequently the current through the switch will drop to zero (see Fig. 2.9b). During off-state period, the voltage over the inductor is dropped to the voltage value over the anti-paralleled diode. (see Fig. 2.9d)

$$v_{L(off-state)} = -V_{diode} \tag{2.4}$$

At $t_{2,}$ the second turn on pulse is fired which causes the current is taken from the lower freewheeling diode to the upper IGBT and the same process is repeated ($i_c = i_L$).

At the time $t_3$ the second turn off pulse is sent to trigger the IGBT gate and the current will stop flowing through the switch.

Regarding the actual application of the test object, the switching losses at the time $t_2$ and $t_3$ are the points of our interest.

# 3 Design theory

In order to perform the single pulse test on the power electronics switches, a "load inductor" is presented in the test circuit which governs the current rise. To avoid the effect of the inductor magnetic field on the test results, the design of the inductor is highly important. The magnetic field outside the existing cylindrical inductor disturbs the waveforms results of the test. At present, a cylindrical inductor plays the role of the load inductor in the test circuit while the magnetic field outside the inductor disturbs the results a lot. Therefore, in order to reduce the disturbance, the inductor has to be placed far away from the measuring probes/devices or it has to be shielded properly.

According to our point of interest, an inductor is simply a passive component in the circuit in order to limit the changes of the current and moderate the electrical flow. The current variation in an inductor is presented according to

$$\frac{di}{dt} = \frac{v}{L} \tag{3.1}$$

Inductance is the property of the circuit element which shows the ability to withstand a variation of the current flow. This property is influenced by the shape, size and material of the core and also the number of turns. First the basic aspects of the inductor design will be presented.

## 3.1 Core

Besides providing the support surface for the winding, the core prepares the medium for the magnetic flux to concentrate and open the path for the flux linkage.

The magnetic flux and magnetic reluctance in a magnetic circuit are analogous to electrical current and resistance in an electric circuit, respectively. A low reluctance core can provide a high flux density.

### 3.1.1 Core characteristics

In this chapter some of the core characteristics will be briefly presented.

### *Permeability*

Permeability of a material is a measure that indicates how well the material can provide magnetic flux from electrical excitation and it presents the capability of the material in conducting the magnetic flux. It shows the ability of the core to concentrate the magnetic field and it is affected by the material and shape of the core [3]. Permeability is measured in $N{\cdot}A^{-2}$ and it is defined by the ratio of the flux density $B$ to the magnetizing force $H$.

$$\mu = \frac{B}{H} \tag{3.2}$$

Permeability is an important parameter of the core which strongly influences the value of the inductance, while a higher permeability provides a higher inductance value. Relative permeability is the ratio of the permeability of a material to the permeability of free space.

$$\mu_r = \frac{\mu}{\mu_0} \tag{3.3}$$

Where $\mu_0 = 4\pi \times 10^{-7}$ $(N{\cdot}A^{-2})$. The multiplication product of the air core inductor value with the relative permeability of the magnetic core material is the inductor value when it is equipped with the core material.

### *Magnetization curve, hysteresis loop*

The core magnetization curve needs to be investigated in order to choose the core material. In Fig. 3.1 the magnetization curve for a typical magnetic core is shown.

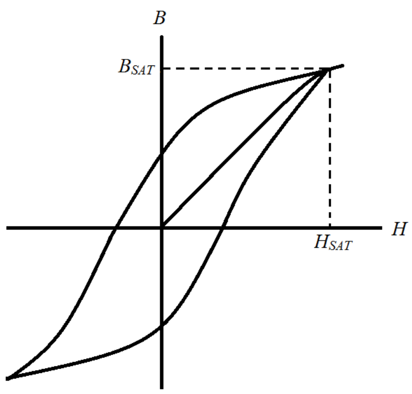


**Fig. 3.1 Magnetization curve**

When a ferromagnetic material is exposed to a magnetic field, it starts to be magnetized, increasing field strength leads to saturation of the flux. Demagnetizing, whether by removing the magnetic field or applying magnetic filed in opposite direction, the material demagnetization path does not follow the magnetization curve. This process introduces the hysteresis loop. The slop of the hysteresis loop is dictated by the permeability of the material which is not constant in a ferromagnetic material. The permeability of the core changes by the field intensity variation since the *B/H* curve is nonlinear. Consequently, generally, it is important to design an inductor with a core material in such a way that the core flux density never approaches the saturation level. In this way, the inductor will operate in the linear portion of the *B/H* curve.

### *Eddy current*

The word eddy is referred to a circular current rotating around a conductor. When an alternating voltage applied to a winding, the magnetic flux is also varying. A current is induced in the material in the vicinity of this varying magnetic flux which produces a magnetic flux opposing the variation of the alternating magnetic flux. This induced current is called eddy current. The magnitude of the eddy current is limited by the core material resistivity [3]. Eddy current easily flows in the material with low resistivity which generates heat in the core and also power losses in transformers. Using thin plates and also lamination of conductors reduce the eddy current losses. These losses are presented in both the inductor winding (conductor) and the core. Using a material with low electrical conductivity would eliminate the eddy current.

### *Quality Factor (Q)*

An ideal inductor is supposed to be purely inductive while it has got no resistive properties. But due to the winding conductor resistance, there is no ideal inductor in the world. The inductor is in series with a resistor which produces heat in the inductor due to the current flow in the winding conductor. Quality factor of an inductor is the ratio of the reactance to the resistance of an inductor.

$$Q = \frac{X_L}{R} \tag{3.4}$$

A higher inductor $Q$ reduces the losses in the inductor.

### 3.1.2 Core material

The core material has a great contribution in the value of an inductor. Generally magnetic materials are presented in three different groups.

**Paramagnetic materials** like aluminum and oxygen, encountering the magnetic field, show almost no magnetic behavior, and they are weakly absorbed by the magnetic field.

**Diamagnetic materials** like cupper, and water, are repelled by the applied magnetic field, their relative permeability $\mu_r$ is less than 1.

**Ferromagnetic materials** like iron, ferrite and magnetite are normally thought of a magnetic material. After magnetization and removing the magnetic field, these materials will retain magnetization. Ferromagnetic materials can be categorized into two different types, soft magnetic materials and hard magnetic materials. Soft magnetic materials are easily demagnetized. But hard magnetic materials need much more energy to be demagnetized. Permanent magnets are made from hard magnetic materials in order to retain the magnetization. Fig. 3.2 shows the hysteresis curve for the hard and soft magnetic materials.

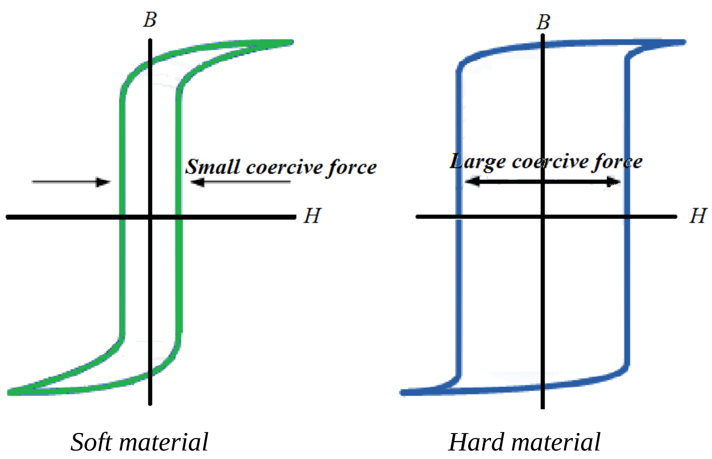


**Fig. 3.2 Magnetic hysteresis loops for soft and hard Materials**

A magnetic field is required in order to demagnetize the magnetic materials and the energy of the magnetic field depends on the coercivity of the material. Coercivity is a measure to show the resistance of a ferromagnetic material to become demagnetized. Hard magnetic materials have a high coercivity and soft materials have a low coercivity. The most common core materials are silicon, iron powder and ferrites which are physically hard and magnetically soft materials.

*Silicon steel*

Silicon steel has a low resistivity property which can easily conduct the electrical current. This property means that the eddy currents can easily flow in the core material which contributes to core losses and heating. Silicon steel has also a low saturation point, i.e. the saturation point is easily reached which decreases the operating range; therefore, the core could not store further magnetic energy.

*Iron powder*

It is made up of iron powder while iron grains are insulated from each other. The air gaps naturally distributed throughout the material provides a distributed air gap effect. The distributed air gap effect introduces the possibility to store higher magnetic flux and also higher dc current before reaching to the saturation point. The resistivity in this material is higher than silicon steel. Iron powder core is rather less costly than the other type of core materials. Furthermore it has a high permeability and resistivity which results in a great reduction of the eddy current throughout the core.

*Ferrite*

A mixture of oxide iron and other elements provides ferrite core which is a magnetic material. Usually it is mixed with manganese zinc (MnZn) or nickel zinc (NiZn) which can be easily magnetized. The main disadvantage of this kind of core is being less robust than other materials. Furthermore the saturation flux density of this material is much less than the one of the powdered metal cores.

Fig. 3.3 shows a comparison of a powdered iron core and a ferrite core with exactly the same core size and winding of the inductors[4].

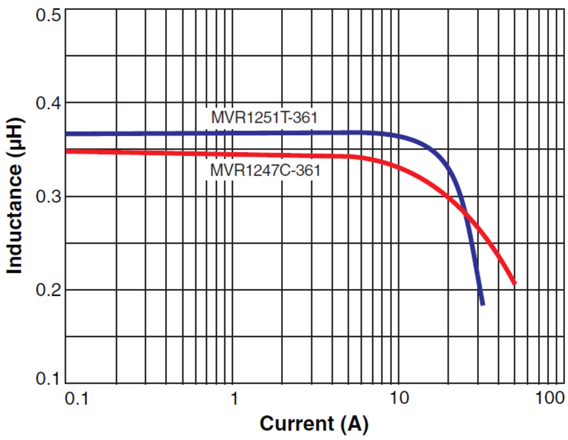


**Fig. 3.3 Comparison of inductance versus current for powered iron(MVR1247C-361) and ferrite(MVR1251T-361) (source: coilcraft)**

The saturation of ferrite and powdered iron core inductors shows that the powder iron core has more gradual saturation characteristics than ferrite. As it is seen, the blue curve (ferrite core MVR1251T-361) drops sooner than the red curve (powder core). This means for higher value of current, powdered iron core is preferred. Table 2 shows the approximate maximum permeability of some common core materials [5].

**Table 2 Approximate maximum permeability of material**

| *Material* | *$\mu (H\ m^{-1})$* | *$\mu_r$* | *Application* |
|---|---|---|---|
| ***Ferrite U 60*** | *1.00E-05* | *8* | *UHF chokes* |
| ***Ferrite M33*** | *9.42E-04* | *750* | *Resonant circuit RM cores* |
| ***Nickel (99% pure)*** | *7.54E-04* | *600* | - |
| ***Ferrite N41*** | *3.77E-03* | *3000* | *Power circuits* |
| ***Iron (99.8% pure)*** | *6.28E-03* | *5000* | - |
| ***Ferrite T38*** | *1.26E-02* | *10000* | *Broadband transformers* |
| ***Silicon GO steel*** | *5.03E-02* | *40000* | *Dynamos, mains transformers* |
| ***Super alloy*** | *1.26* | *1000000* | *Recording heads* |

Relative permeability ($\mu_r$) shows the ratio of the flux density of the material and of the situation when the same magnetic field applied to a vacuum. For example the relative permeability for *Ferrite U 60* is *8* which means if the same field strengths applied to the vacuum the magnetic flux density will be 8 times less than the one of *ferrite U 60* core material. $\mu_r$ is not constant and it changes with the field strength and the flux density variation and also with temperature. In the Table 2 the "maximum" permeability of the materials are shown.

*Ceramic and air*

Since ceramic has no magnetic properties, from the magnetic point of view a ceramic core is assumed as an air core. This core material is used in high frequency applications where a low inductance value is required. In order to provide a higher inductance value, a higher number of turns are needed and the coil has to be very long.

By using an air core inductor, the weight and cost of the core would be eliminated. Furthermore the problem of magnetic saturation, the variation of the permeability of the core with the temperature variation and also the nonlinearity of the *B-H* curve will be avoided [6],[7],[8].

### 3.1.3 Core shape

In order to improve the SPT circuit and design the new load inductor, a brief study and investigation of the different shapes of inductors is necessary. The shape of an inductor core is designed considering the required inductance value, the cost, the inductor role in the circuit and also the ease of winding process.

*Cylindrical core*

A cylinder provides a stand for the winding. The material of the cylinder, the number of winding turns and the length of the cylinder introduce the inductor value.

*Toroidal core*

Winding on a donut shaped surface is called a toroidal inductor. This kind of core is good in self-shielding while one of the most important advantageous of the toroidal inductor is the concentration of the magnetic field "inside" the inductor and almost no outside radiation occurs.

## 3.2 Winding

Usually the wire winding in an inductor is insulated to avoid short out in adjacent turns which are closely wound. The number of winding turns is limited by the inner diameter in a toroidal inductor or by the length of the cylinder in a cylindrical inductor. In order to reach to a higher inductance value, multiple layers of winding are needed. While choosing a larger core also makes a contribution.

## 3.3 Inductance formula

There are factors which affect the value of an inductor:

- **Number of turns**: The higher number of winding turn provides higher value of inductance in an inductor. The inductor can generate a greater amount of magnetic field force with more number of turns.

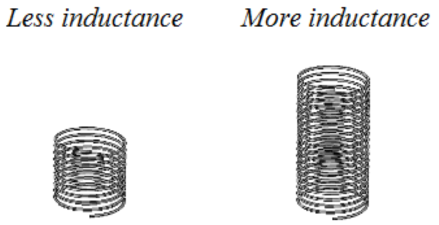


- **Coil area:** Greater coil area provides a greater inductance value. Less opposition to the magnetic field formation is presented by the greater coil area.

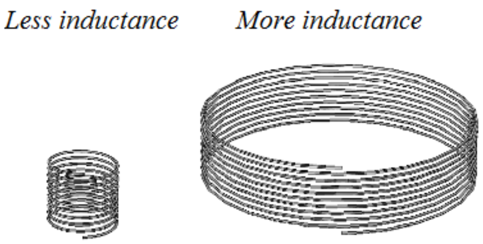


- **Coil length:** The longer the coil length the less inductance. When the core is longer, the magnetic field flux has a longer path to take which results in more and more opposition to the formation of the flux.

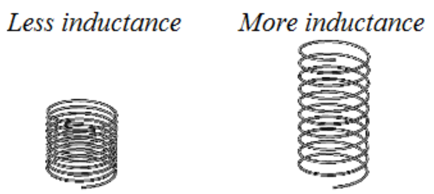


- **Core material:** Core material also has a large effect on the inductance value. The magnetic permeability of the core material influences the inductance value. The higher permeability provides a greater inductance while providing greater magnetic field flux.

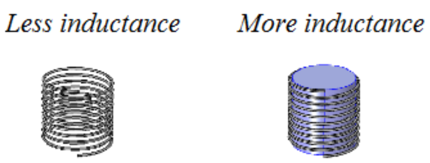

According to the aforementioned tips, the formula for almost any coil of wire is presented as

$$L = \frac{\mu N^2 A}{l} \tag{3.5}$$

where

$L$: Coil inductance (Henry)

$N$: Number of coil wire turns

$\mu$: Core material permeability

A: Coil area ($m^2$)

$l$: Coil length (m);

And the inductance of a toroidal inductor is given by

$$L = \frac{\mu N^2 h}{2\pi} ln\left(\frac{r_b}{r_a}\right) \tag{3.6}$$

where

$h$: Toroid thickness

$N$: Number of the winding turn

$r_b$: Outer radius of the toroid

$r_a$: Inner radius of the toroid.

If there is a core material instead of air core, then the calculated inductance needs to be multiplied by the relative magnetic permeability of the core material.

# 4 Inductor design

A toroidal inductor is chosen to be designed in order to reduce the magnetic field spreading outside the inductor, which contributes to decrease the disturbances in the test circuit and improve the measurement results of the single pulse test.

## 4.1 Core material

Besides preparing the medium for the magnetic flux to concentrate and open the path for the flux linkage, the core provides the support surface for the winding. Designing an inductor, side effects of the core material properties should be considered. Due to eddy currents and hysteresis, applying a time varying current to the inductor produces a time varying field which leads to energy losses in the form of heat dissipation in the core. A drawback of using a ferromagnetic core appears when a high current is applied to the inductor which could saturate the core and the inductance value fluctuates by the current variation. Air core is a proper material in our project but a form needed to put the winding on it. In order to avoid the saturation and the inductance variation issues, cores made of material like wood, paper, glass and ceramics, which are dielectric materials, are considered in our case. Manufacturing a “donut” shape configuration for the toroidal core should also be taken into account. Consequently, wood is chosen for the core material. Choosing wood as core material is a proper selection since the permeability of wood is similar to the one of air. Table 3 shows the properties of the American red oak which is taken from COMSOL Multiphysics® Material Library.

**Table 3 Wood magnetic properties**

| ***Property*** | ***Name*** | ***Value*** |
|---|---|---|
| *Relative permeability* | *Mur* | *1* |
| *Electrical conductivity* | *Sigma* | *2.857e-18[S/m]* |
| *Coefficient of thermal expansion* | *Alpha* | *4.9e-6[1/K]* |
| *Relative permittivity* | *Epsilon* | *2* |
| *Density* | *Rho* | *630[kg/m^3]* |

As it is seen the relative permeability of the wood is 1. The actual value of the relative permeability of wood is 1.00000043 *[5]* which is so close to air 1.00000037*[9]*. Furthermore, the low electrical conductivity of wood contributes to elimination of the eddy current in the core.

## 4.2 Core size, winding and conductor cable

According to the inductance value and the space available for the inductor, the core size is designed. Inner diameter of the toroidal core is restricted by the first layer number of turns and certainly with the radius of the conductor. Consequently, the core inner radius is given by

$$r_i = \frac{ND}{2\pi} \tag{4.1}$$

where

$r_i$: Inner radius(mm)

$N$: number of turns on the first layer

$D$: Conductor diameter(mm).

Considering the short time current flow in the conductor, the cross section of the cable including the isolation is chosen to be 10mm². The cable size has no effect on the inductance value but it affects the series resistance of the toroid.

In this design two core sizes are considered and after making a comparison, the proper one is selected. The inner diameter of the small inductor is 17cm while the diameter of the large inductor is 25cm. Fig. 4.1 and Fig. 4.2 show the variation of the inductance with the outer diameter variation while the inner diameter is kept constant.

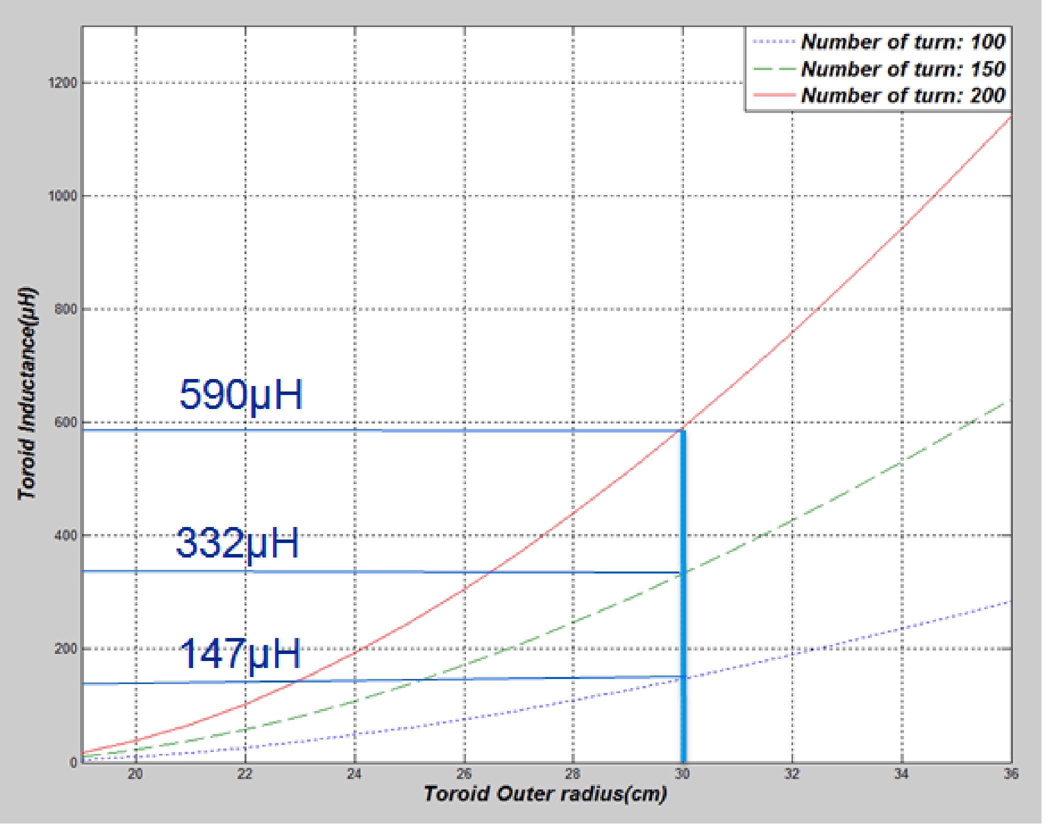


**Fig. 4.1 Inductance variation versus variation of the outer radius of the Toroid($r_{inner}$=17cm)**

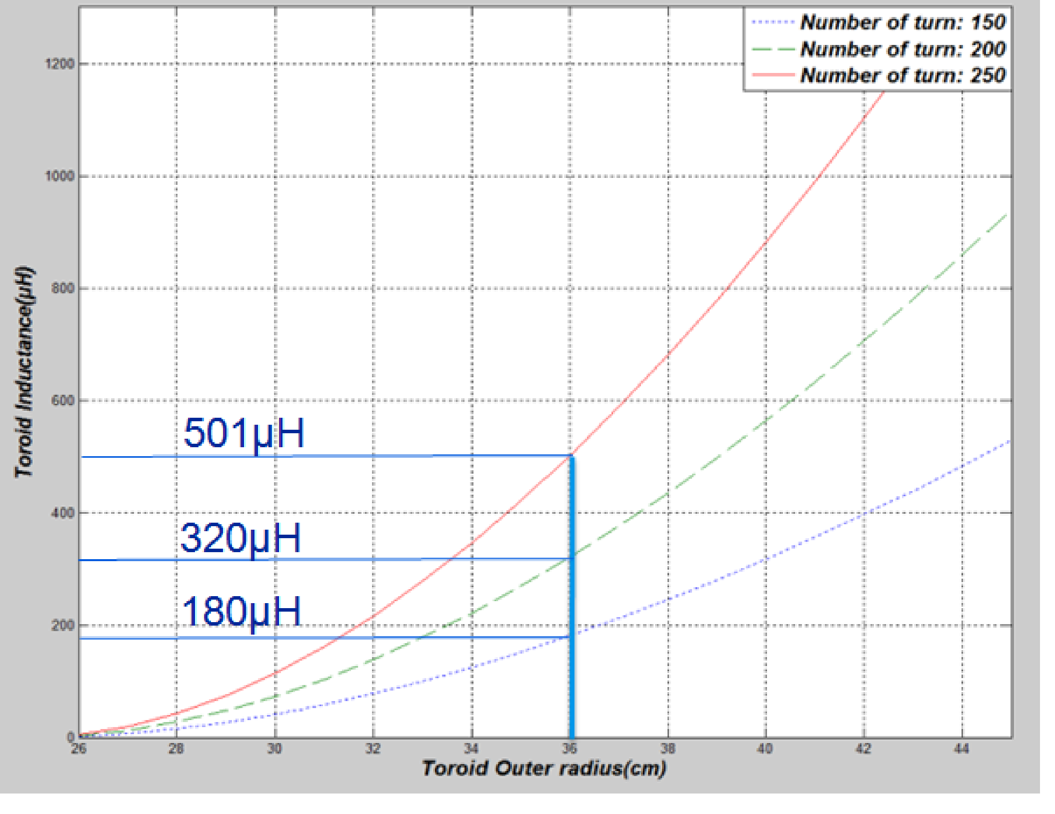


**Fig. 4.2 Inductance variation versus variation of the outer radius of the Toroid ($r_{inner}$=25cm)**

Each inductor in this design has three different cable ends which provide three different inductance values. In Fig. 4.1, the variation of the “small inductor” is shown. Considering 30cm outer radius, the first end provides 147µH which is made up 100 turns on the first layer. The second end produces 332µH which is consist of 100turns on the first layer and 50 turns on the second layer. There is still some space left empty between the adjacent turns of 50 turns on the second layer in order to provide a homogenous magnetic field. The remaining space is filled by another 50turns on the second layer which produces 590µH.

Fig. 4.2 shows the inductance variation of the “large inductor”. Inner radius of this toroid is 25cm while considering 36cm for outer radius provides 180µH consists of 150turns on the first winding layer. The second layer is made up by two 50-turns parts. The first 50-turns together with the first layer 150turns provide 320µH while adding another 50turns on the second layer provides 500µH in total.

Taking into account the various required inductance values in the SPT circuit and the diameter of the cable conductor, the small toroid is chosen. Consequently this inductor is able to provide 3 different inductance values which could be applied in three different tests according to the required inductance value which is defined based on the test object.

Designing and operation of the multilayer winding inductor is sophisticated due to the parasitic capacitance between the layers likewise between the adjacent windings. In order to avoid these challenges the layers need to be isolated with some kind of shield such as Mylar film.

## 4.3 Inductance

Regarding the aforementioned considerations, a multi-inductance value toroid is designed which could provide 147µH, 332µH and 590µH. In this approach, the inductor would be applicable in various tests for different test objects.

## 4.4 Inductor resistance

It is also important to know the resistance of the inductor, since it comes up to the voltage drop over the inductor and likewise the voltage drop over the anti paralleled diode (see Fig. 2.10 and Fig. 2.11). The series resistance of the inductor is defined by the length of the cable.

## 4.5 Magnetic field

The point of interest in this thesis is to reduce the spreading magnetic field and to reduce effect of the magnetic field disturbance on the test results. The magnetic field measurement is presented in chapter 7.3.

## 4.6 Eddy current and Hysteresis

Air is chosen for the core material and wood is selected for the winding-stand, which help to eliminate the eddy current in the core and solve the hysteresis and saturation problems due to the very low electrical conductivity.

## 4.7 Temperature

However the current passing through the inductor is very high, the temperature rise in the inductor is negligible since the duration of conduction is a fraction of a millisecond.

# 5 Model simulation in COMSOL Multiphysics®

Why a toroidal inductor, not a common cylindrical inductor? In order to picture the improvement of the inductor, a simulation is performed in COMSOL Multiphysics® for both the existing cylindrical inductor and the designed toroidal inductor. COMSOL Multiphysics® is easy-to-use software for modeling and simulation of real world multi-physics systems [10]. The simulation is performed in COMSOL Multiphysics® 4.3a. AutoCAD 2011 also used in order to sketch a model of the toroidal inductor which was impossible to be drawn in COMSOL Multiphysics®.

## 5.1 Existing cylindrical inductor

A “3D” space dimension is selected in order to provide a better demonstration and clear comprehension of the simulation. “Magnetic fields” physics is chosen in order to study the magnetic field produced by the inductor. An inductor is modeled based on the actual cylindrical inductor geometries in the single pulse test circuit. But in order to provide the same inductance value in COMSOL Multiphysics® as the inductor in the circuit, slight changes are made in the geometry and the number of turns. Table 4 shows the final Geometry and inductance value of the cylindrical inductor modeled in COMSOL Multiphysics®.

**Table 4 The final COMSOL Multiphysics® modeled inductor geometry**

| | |
|---|---|
| ***Number of turns*** | *44* |
| ***Radius*** | *15cm* |
| ***Height*** | *44cm* |
| ***Inductance*** | *280.4 µH* |

In order to produce a model with the same inductance value as the actual inductor, the geometry of the cylindrical inductor is slightly changed in COMSOL Multiphysics®. The Cylindrical inductor modeled in COMSOL Multiphysics® is pictured in Fig. 5.1.

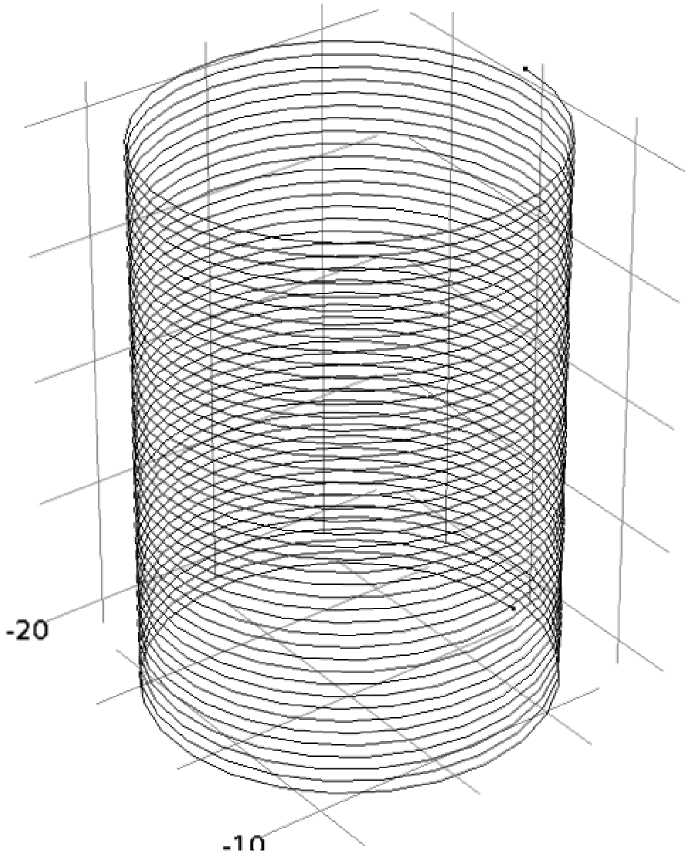


**Fig. 5.1 Cylindrical inductor modeled in COMSOL Multiphysics®**

An air core inductor is modeled in COMSOL Multiphysics® while the core in the actual inductor is made up polypropylene cylinder. The diameter of the conductor is not considered in the modeled inductor whilst an edge of current introduces the cable conductor.

Considering the current applied to the inductor in the single pulse test circuit and equation (3.1) , the current through the inductor increases from 0 to 1.8 kA during 173µs. consequently a “time dependent” is selected in COMSOL Multiphysics® and the following current waveform is applied to the inductor,

$$i_L = \frac{1800(A)}{173(\mu s)} t \qquad (5.1)$$

In order to verify the applied current to the modeled inductor, the current waveform is drawn in COMSOL Multiphysics® which is shown in Fig. 5.2.

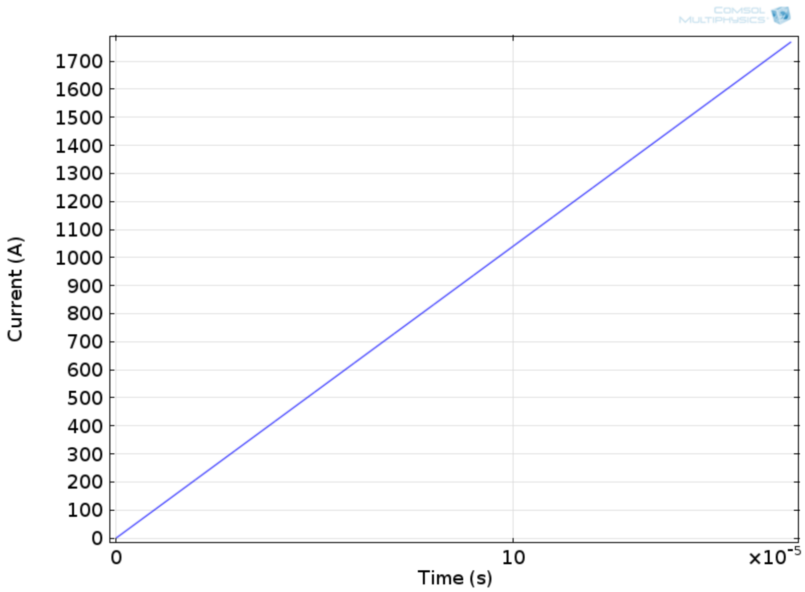


**Fig. 5.2 Current applied to the inductor**

The direction of the current in the inductor is shown in Fig. 5.3.

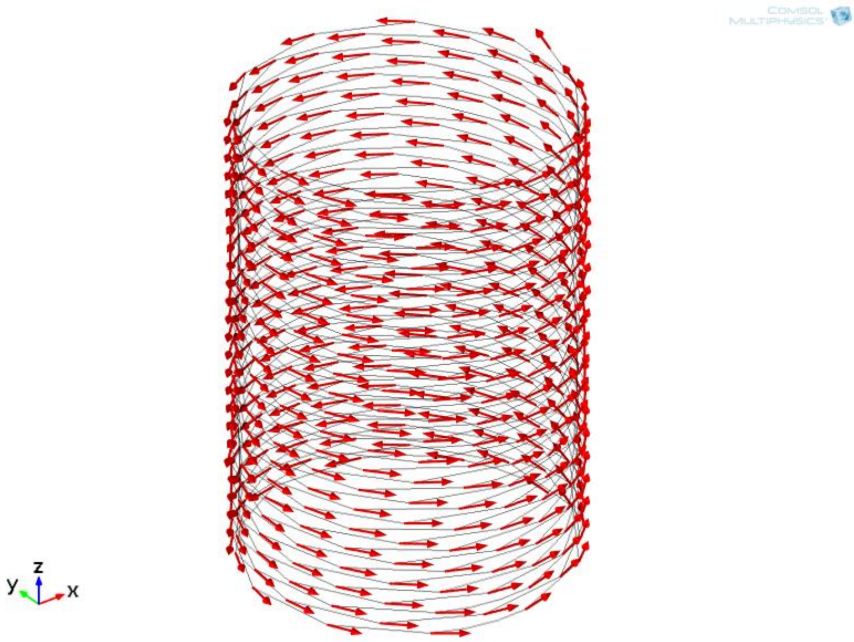


**Fig. 5.3 Current direction in the inductor modeled in COMSOL Multiphysics®**

The current has a counterclockwise direction. According to the right hand rule, from the current direction in the inductor, the direction of the magnetic field is expected to be upward inside the cylinder, and downward outside the cylinder.

A sphere of air is considered around the inductor which is needed to study the parameter in the vicinity of the inductor. Fig. 5.4 shows the model inside a sphere.

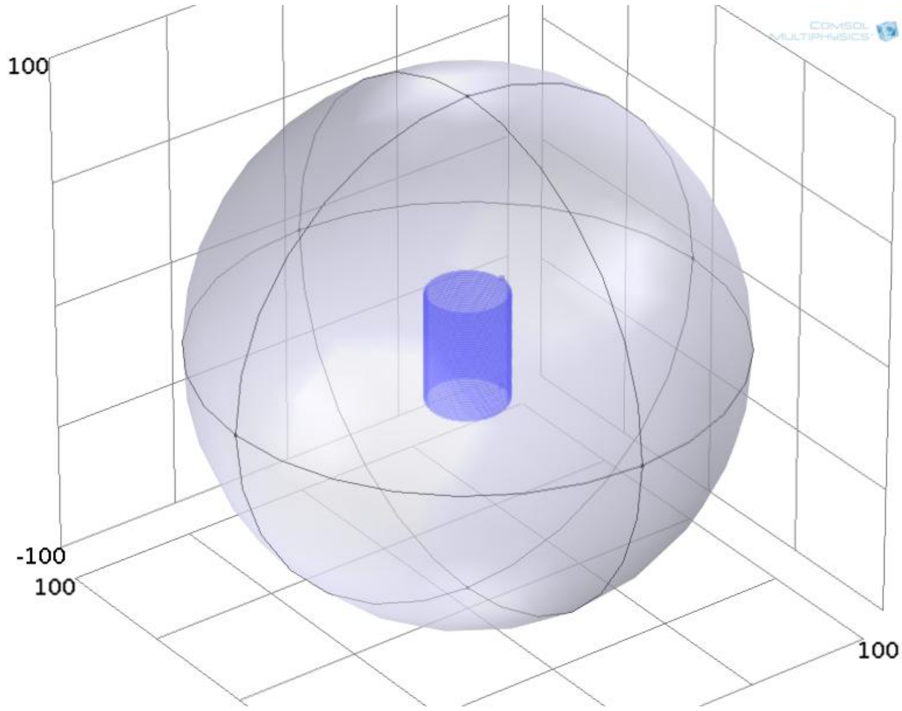


**Fig. 5.4 Cylindrical inductor modeled in COMSOL Multiphysics® including the sphere**

A 1-meter diameter sphere is sketched around the inductor in order to provide the possibility to investigate the magnetic field around the inductor.

In order to calculate the inductance, in COMSOL Multiphysics®, the energy equation is applied,

$$W_m = 1/2 \times LI^2 \tag{5.2}$$

To calculate the energy density "surface integration" is implemented besides using the "volume integral".

$$W_m = \iiint W_m \, dv \tag{5.3}$$

According to COMSOL Multiphysics® estimation the inductance is equal to

$$L_{Cylindrical} = 277 \mu\text{H}$$

After implementing values for the time variation (0-173μs), the program starts to compute the model. In this project, reducing the magnetic field spread is a point of interest. So the magnetic flux and magnetic density around the inductors need to be estimated. The magnetic field and the direction are pictured in Fig. 5.5 and Fig. 5.6.

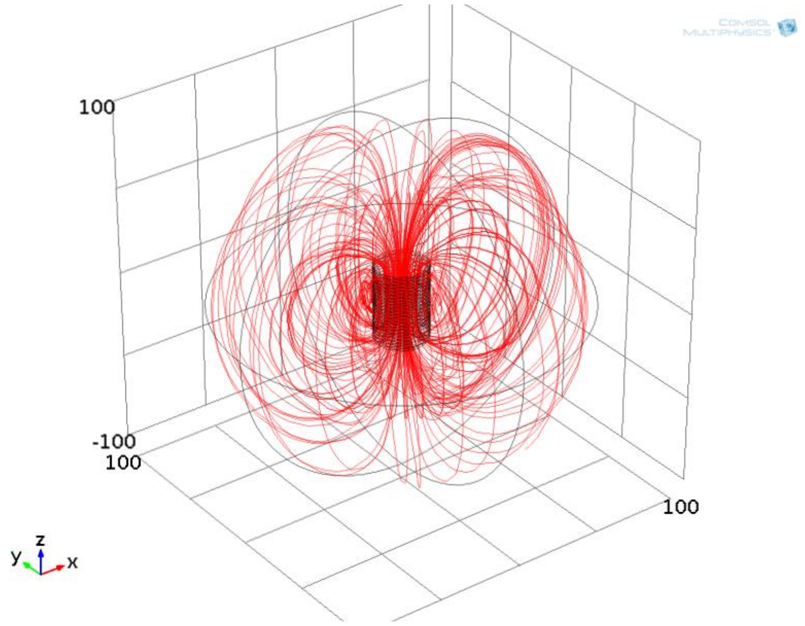


**Fig. 5.5 Magnetic field lines**

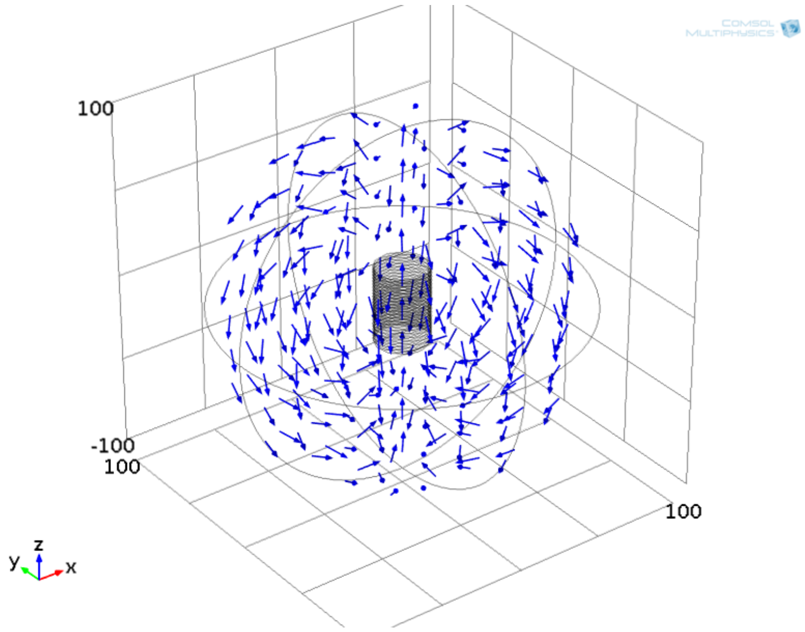


**Fig. 5.6 Magnetic field direction**

As it is expected, the magnetic field arrows are upward inside the cylinder and they are downward outside the cylinder, which is based on the current direction and it is in accordance with the right hand rule.

In order to estimate the magnetic field values in the vicinity of the inductor, 3D lines are needed, which are shown in Fig. 5.7 and Fig. 5.8.

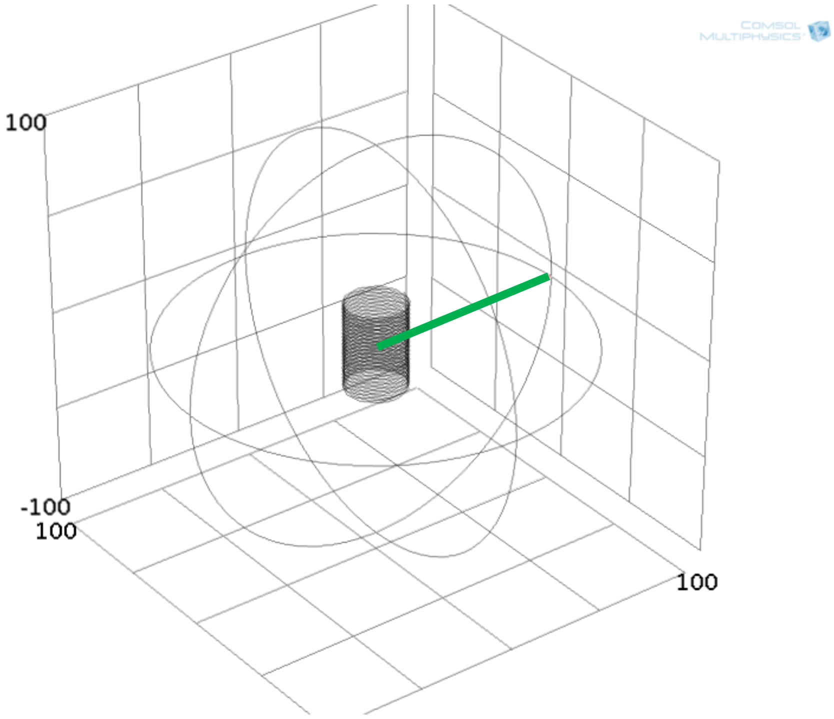


**Fig. 5.7 Cutline 3D 1**

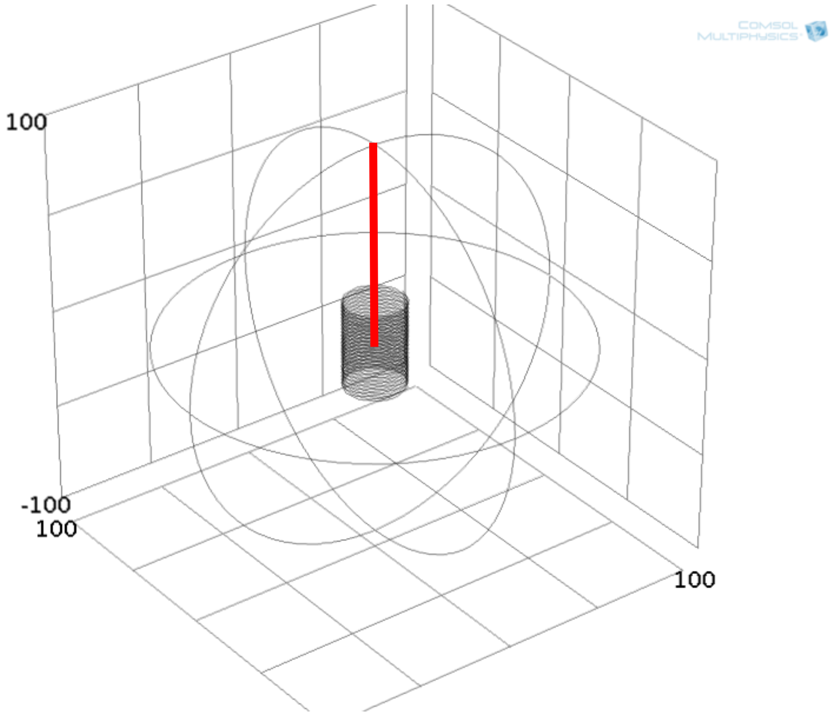


**Fig. 5.8 Cutline 3D 2**

Fig. 5.7 shows Cutline 3D 1 which is horizontally drawn from the “center point” of the inductor to 1m away. Fig. 5.8 shows Cutline 3D 2 which is vertically sketched from the “center point” to 1m away above the inductor.

The magnetic flux density[2] on the Cutline 3D 1 and 2, at the t = 173μs, is shown in Fig. 5.9, while the highest current is applied to the inductor and the magnetic field is maximum.

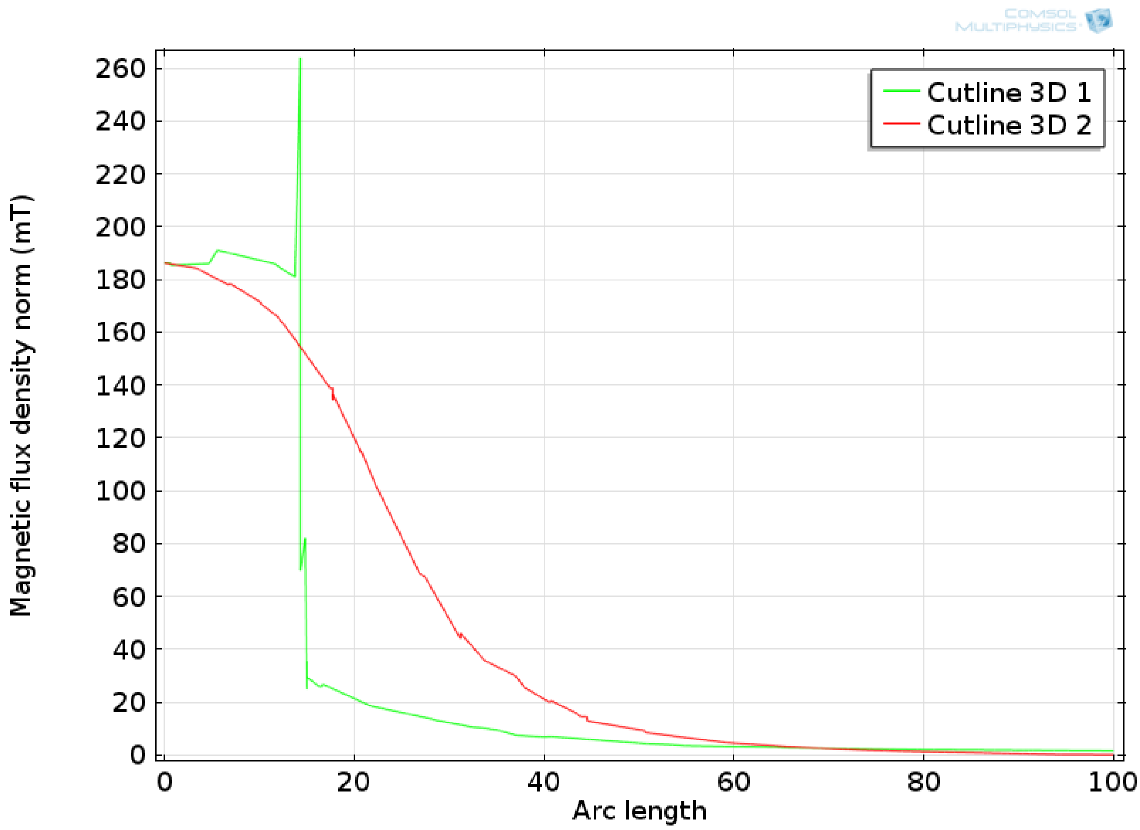


**Fig. 5.9 Magnetic field (magnetic flux density) on the Cutlines(t=173μs)**

Considering cutline 3D 1, the magnetic field is rises when the line passes on the conductor winding and it decreases dramatically outside the inductor while the magnetic field on cutline 3D 2 gradually and smoothly decreases. The magnetic field value on cutline 3D 1 is much lower than cutline 3D 1, considering the points close to the winding.

---

[2] Magnetic flux density of 1 Wb/m² is 1 Tesla, which is called magnetic field.

In order to study the magnetic field variation outside the inductor, cutline 3D 3 and cutline 3D 4 are introduced which are drawn from the “conductor winding” away to the side and above the inductor, respectively. Fig. 5.10 and Fig. 5.11 show cutline 3D 3 and cutline 3D 4.

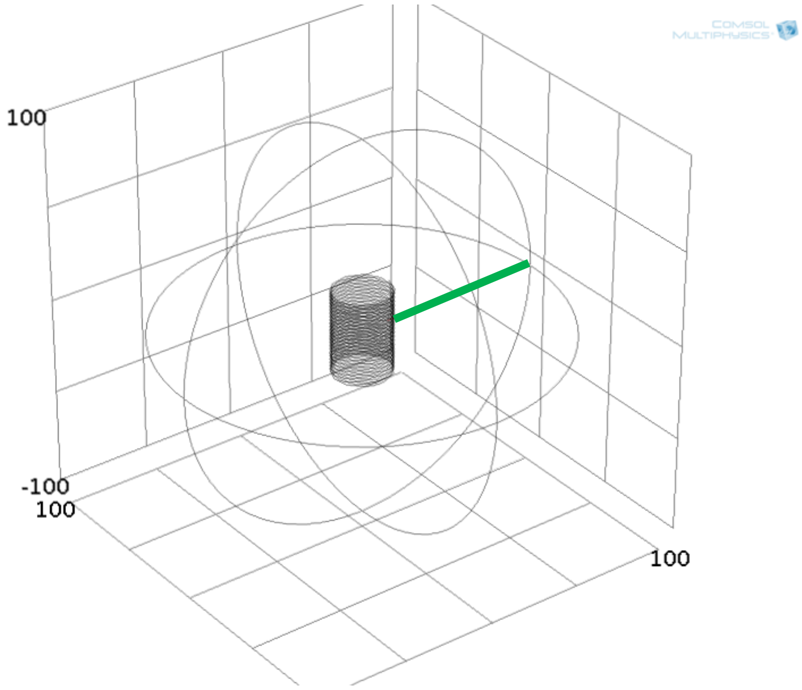


**Fig. 5.10 Cutline 3D 3**

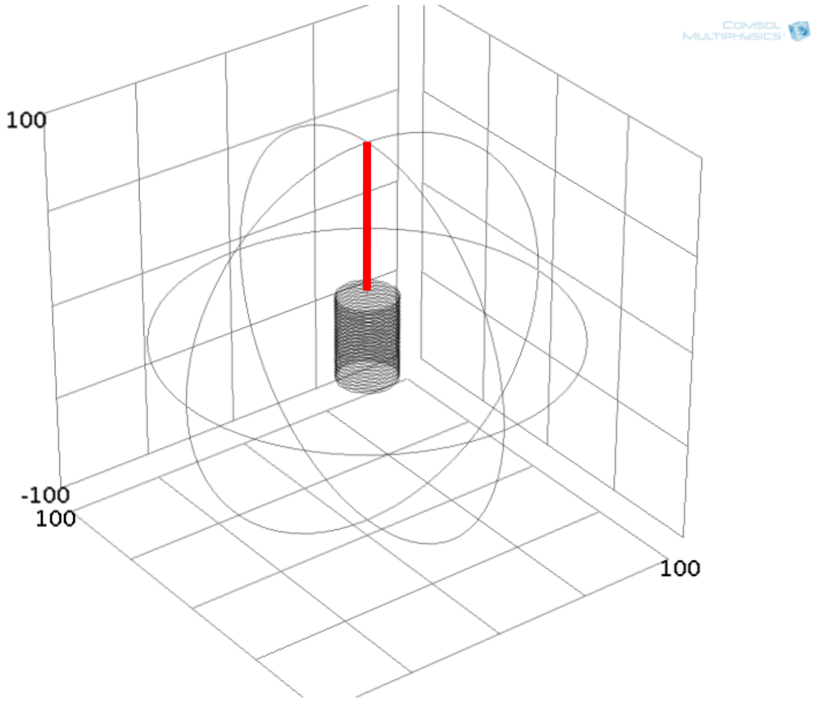


**Fig. 5.11 Cutline 3D 4**

Magnetic field on the Cutline 3D 3 and Cutline 3D 4 are pictured in Fig. 5.12.

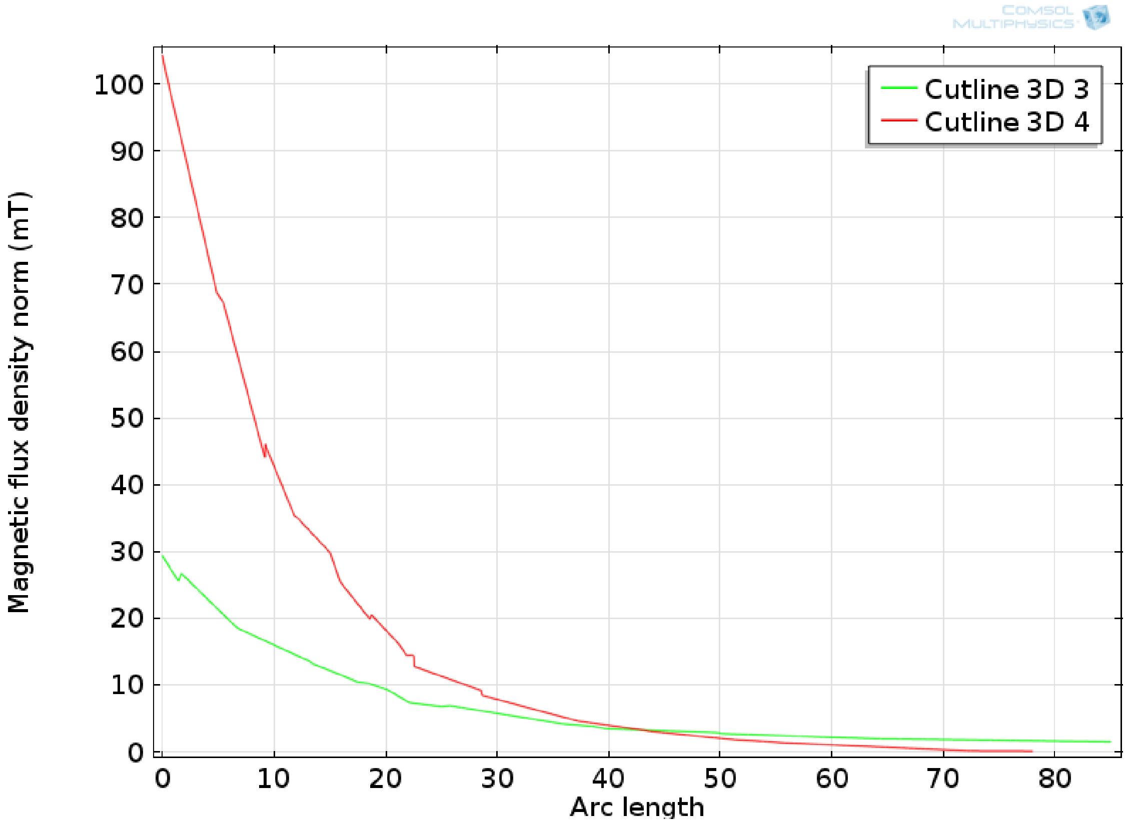


**Fig. 5.12 Magnetic field on Cutlines started from the conductor winding to the side and above the inductor (t=173μs)**

As it is seen, up to about 40cm away from the inductor, the magnetic field on Cutline 3D 3 is much higher than the one on Cutline 3D 4. Furthering away from the inductor, the magnetic field is reduced. The magnetic flux density at different distance away from the inductor is shown in Table 5.

**Table 5 Magnetic flux density around the cylindrical inductor**

| *Length (cm)* | *5* | *10* | *15* | *20* | *25* | *30* | *35* | *40* | *45* | *50* | *55* | *60* | *65* | *70* |
|---|---|---|---|---|---|---|---|---|---|---|---|---|---|---|
| *$B_{Cutline3D\ 3}$ (mT)* | *21.308* | *15.999* | *12.154* | *9.377* | *6.764* | *5.755* | *4.413* | *3.432* | *3.131* | *2.698* | *2.437* | *2.163* | *1.898* | *1.819* |
| *$B_{Cutline3D\ 4}$ (mT)* | *67.901* | *42.798* | *29.886* | *18.248* | *11.302* | *7.837* | *5.598* | *3.954* | *2.827* | *2.007* | *1.410* | *1.015* | *0.669* | *0.304* |

Increasing the distance away from the inductor, reduces the magnetic field spreading. As it is observed, considering up to 40cm away from the inductor winding, the magnetic field above (on Cutline 3D 4) the inductor is much higher than the magnetic field beside it (on Cutline 3D 3). But if further than 40cm is considered, the magnetic on cutline3D 4 is less than the magnetic field on cutline3D 3. This can be concluded that the magnetic field in the vicinity of the inductor, close to the winding, is more cancelled out in the sides of the inductor than above it. This cancellation of the magnetic field is made by the effect of the diverse current direction in two sides of the cylinder. Magnetic field cancelation is reduced by increasing the distance. Fig. 5.13 and Fig. 5.14 verify the aforementioned conclusion.

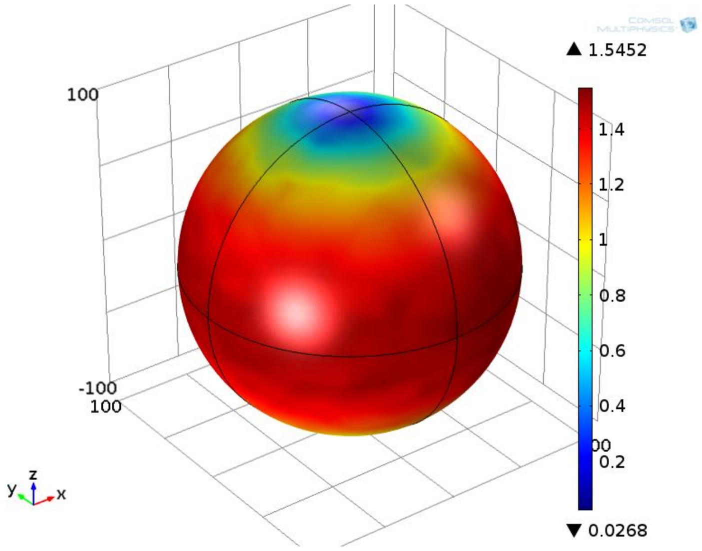


**Fig. 5.13 Magnetic field[mT] on the surface of a 1m-radius sphere around the inductor at t=173μs**

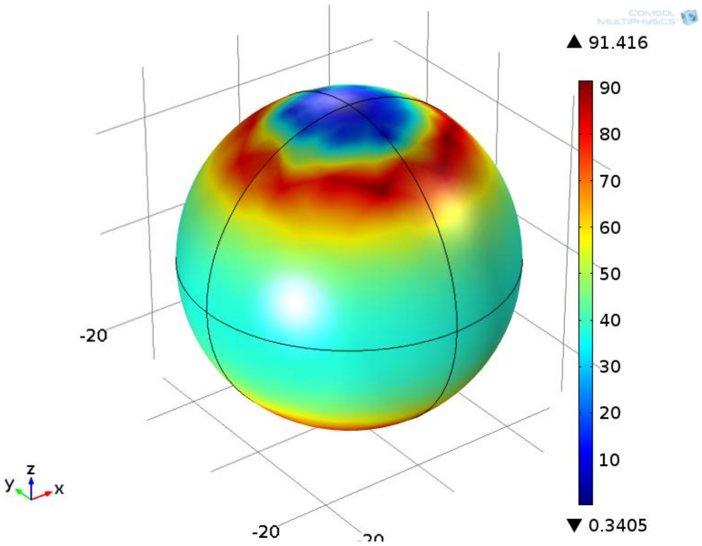


**Fig. 5.14 Magnetic field[mT] on the surface of a 30cm-radius sphere around the inductor at t=173μs**

In Fig. 5.13 the radius of the sphere around the inductor is 1meter. The magnetic field on the side surface is higher than the above surface while in Fig. 5.14 the magnetic field in the side area is lower than the above area, since the radius of the sphere is 30cm and the surface is closer to the winding.

## 5.2 Designed Toroidal inductor

The smaller designed toroid is selected for the simulation. In order to have a similar inductor value in both models, 150truns is chosen for the toroidal inductor which provides 284µT while the cylindrical inductance value is 280µT.

There is no straight way to sketch a model of the actual toroidal inductor in COMSOL Multiphysics®. The only way to do so is to draw the model in other program and then import it to COMSOL Multiphysics®. Fig. 5.15 shows the model sketched in AutoCAD which is imported to COMSOL Multiphysics®.

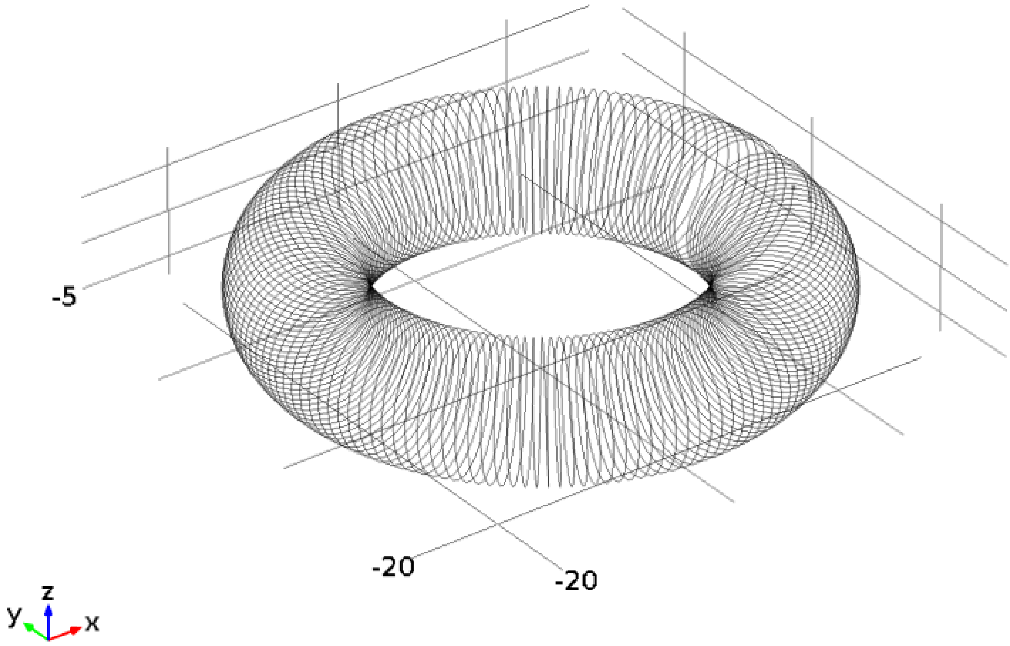


**Fig. 5.15 Designed toroidal inductor modeled in COMSOL Multiphysics®**

The properties of this inductor are according to Table 6.

**Table 6 Simulated inductor properties**

| ***Property*** | ***Value*** |
|---|---|
| *Inner radius* | *16cm* |
| *Outer radius* | *30cm* |
| *Number of turns* | *150* |
| *Winding conductor material* | *Copper* |
| *Inductance* | *284.8296 µH* |

The same procedure needs to be performed to make the model ready for the computation and the same current as the previous model is applied to the inductor. Fig. 5.16 shows the direction of the current applied to the inductor.

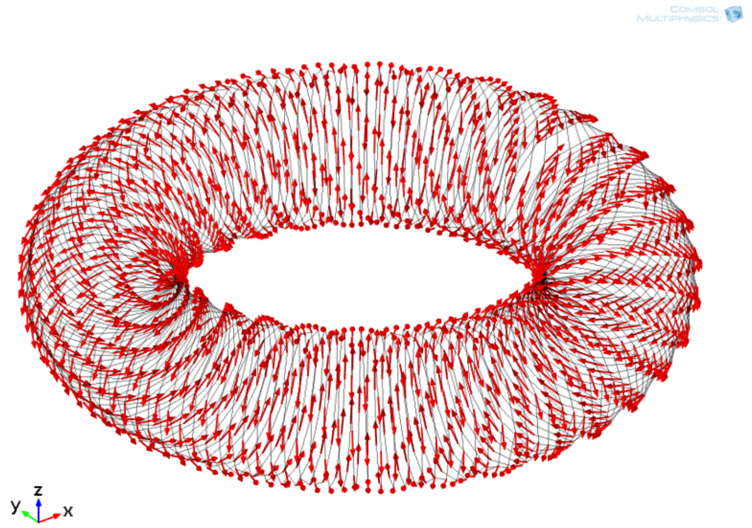

**Fig. 5.16 Direction of the current applied to the inductor**

As it is seen, the current goes up in the inner part and it goes down in the outer part. The figure is taken at $t = 173\mu s$ while the highest current value applied to the inductor which is 1.8KA. According to the current direction, magnetic field direction inside the toroid is predictable. The direction of the magnetic field inside the toroid is supposed to be counter clock wise viewed from above. Fig. 5.17 shows the magnetic field direction inside the toroid.

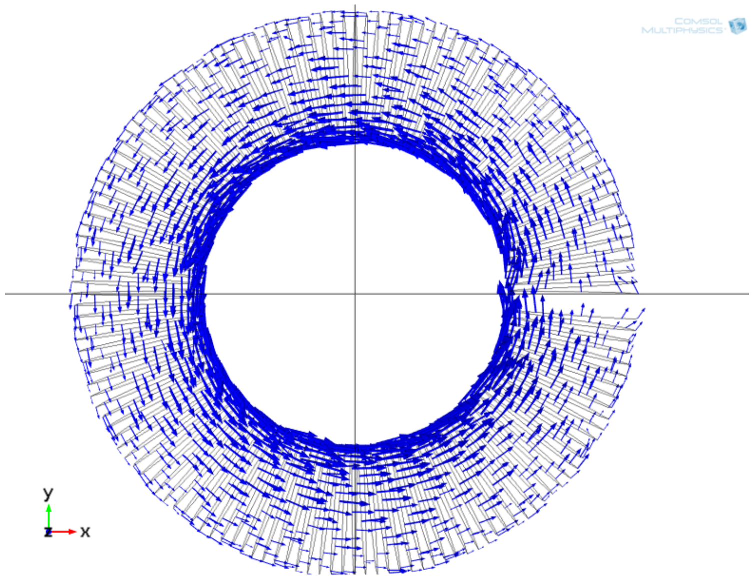

**Fig. 5.17 Magnetic field inside the toroid(view from above)**

As it is demonstrated, the magnetic field is relatively concentrated inside the toroid. The magnetic field in the inner part is higher since the winding turns are closer to each other and the current is denser. But in the other surface the magnetic field is lower since the distance between two adjacent turns is longer.

Magnetic field outside the toroid is point of interest in this work. Researches and studies have proven that the magnetic field outside the toroid is much lower than the one inside. The magnetic field in the vicinity of the inductor is shown in Fig. 5.18.

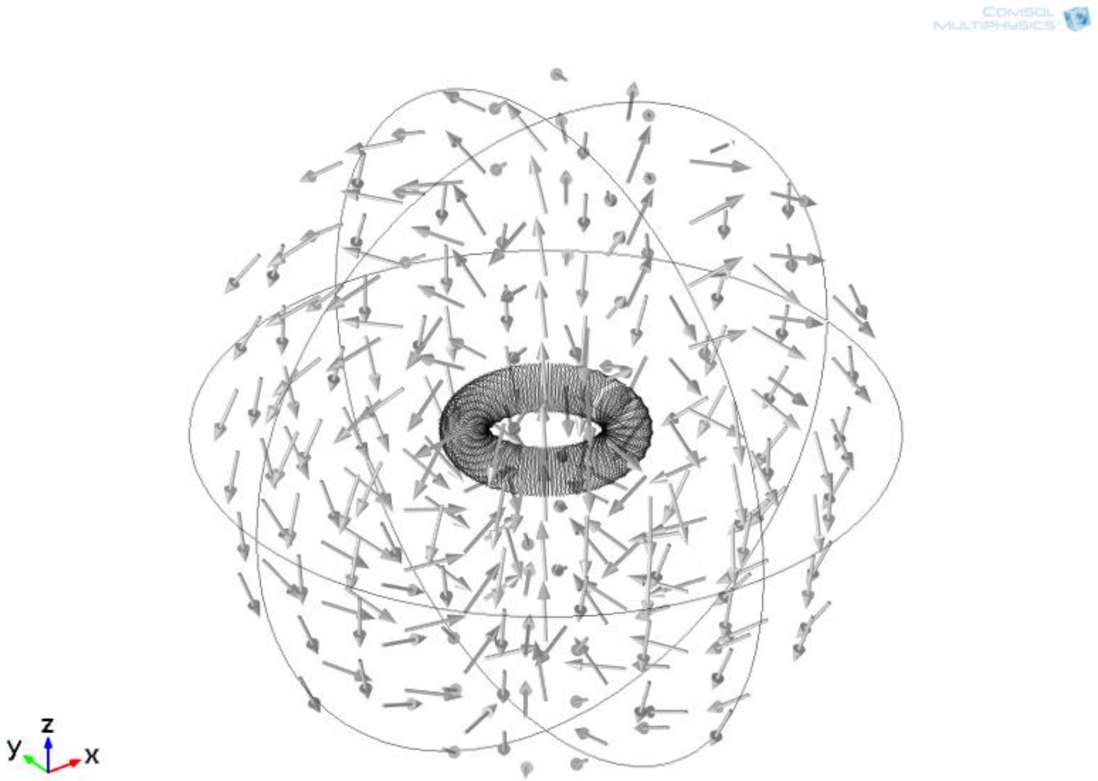


**Fig. 5.18 Magnetic field around the inductor**

The magnetic field goes up in middle of the toroid and it goes down in the outside part. The direction of the current is counter clockwise viewed from above which explains the direction of the outside magnetic field. Magnetic field on the surface of a 2meters diameter sphere around the inductor is shown in Fig. 5.19.

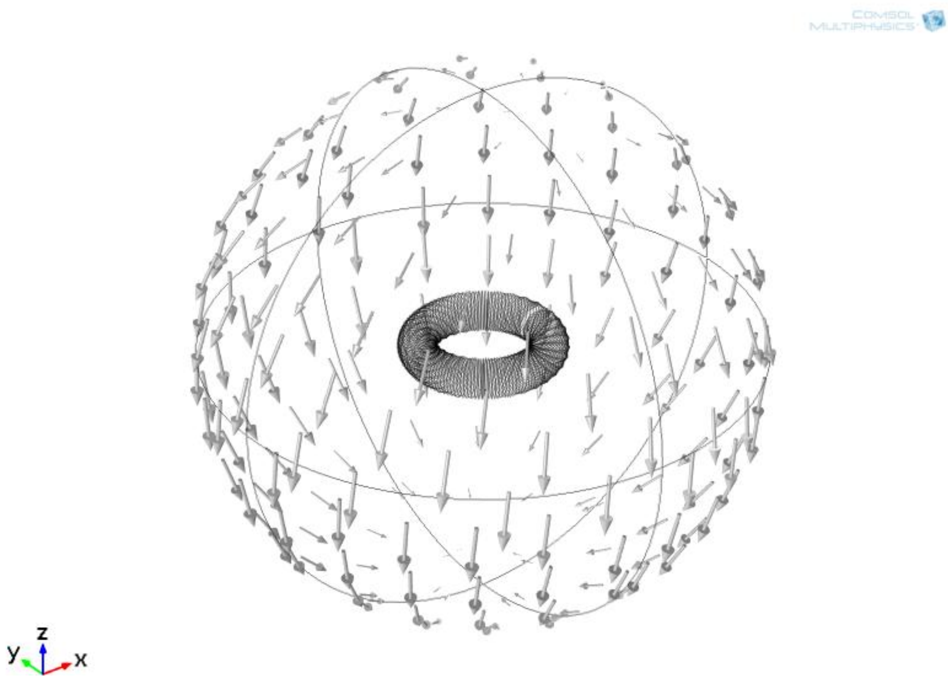

**Fig. 5.19 Magnetic field on the surface of a 2 meters diameter sphere around the inductor**

As it is clearly seen the magnetic field is downward in the outer part of the inductor which is in accordance with the direction of the current.

Cutline 3D 1 and Cutline 3D 2 are drawn in order to estimate the magnetic field around the toroid which are shown in Fig. 5.20 and Fig. 5.21.

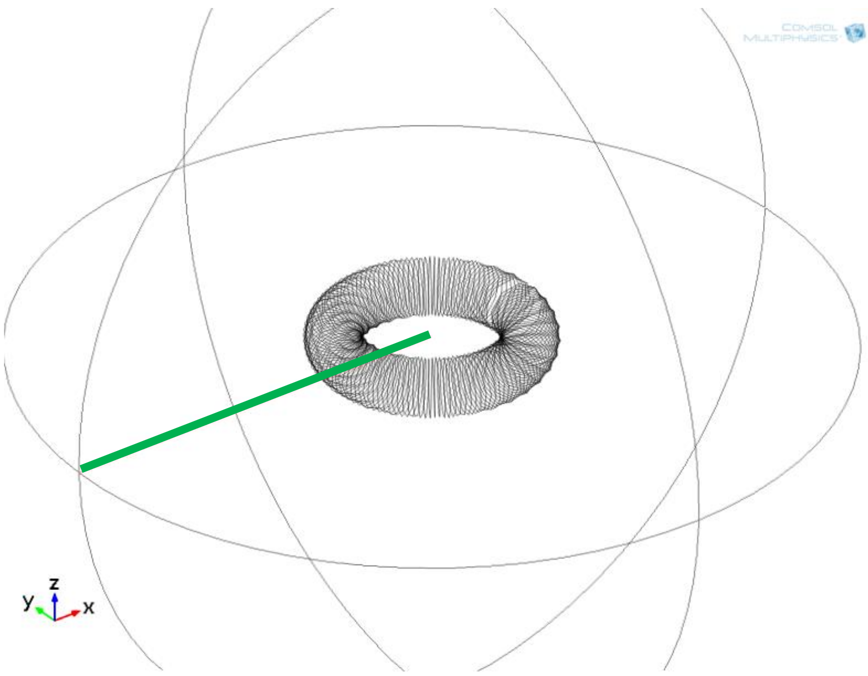

**Fig. 5.20 Cutline 3D 1**

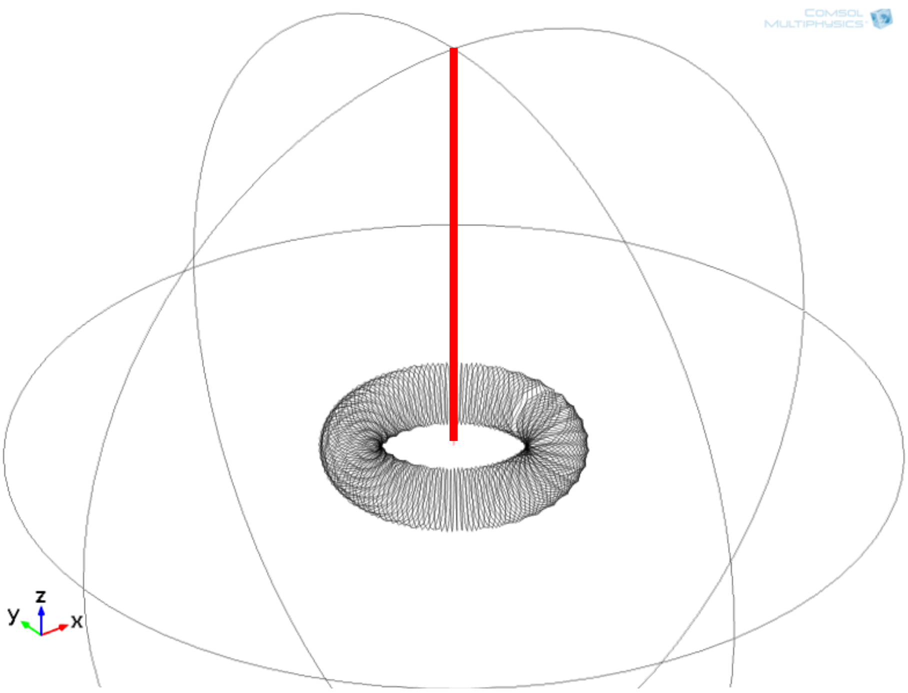


**Fig. 5.21 Cutline 3D 2**

Cutline 3D 1 is drawn horizontally from the center point of the inductor to 1m away and Cutline 3D 2 is vertically sketched from the center point to 1m above the inductor. The magnetic flux density (magnetic field) on Cutline 3D 1 and Cutline 3D 2, at the t = 173 μs, when the highest current value passes through the inductor, is shown in Fig. 5.22.

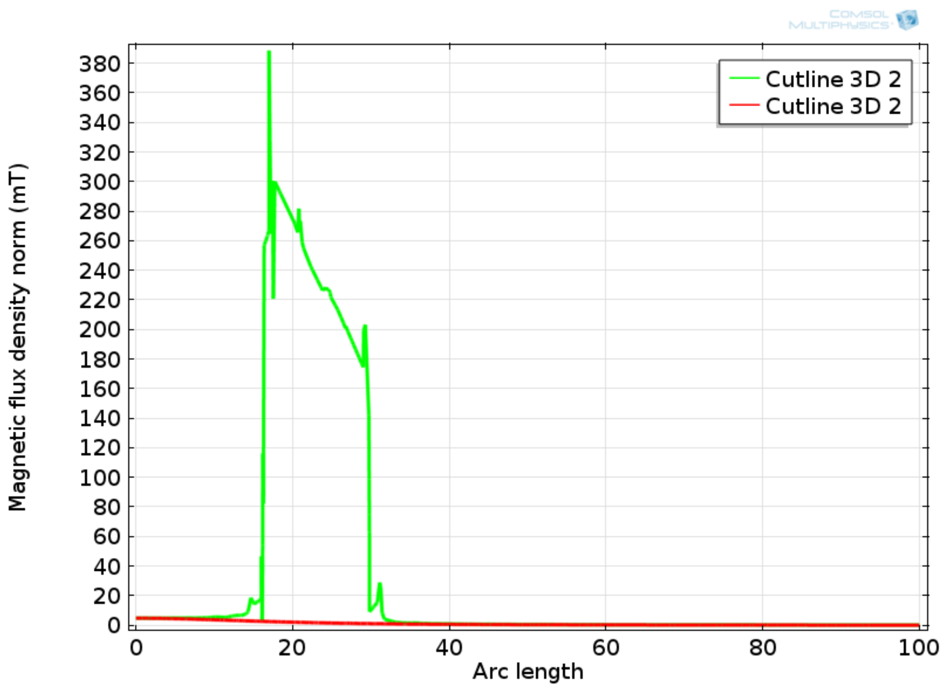


**Fig. 5.22 Magnetic flux density(magnetic field) on Cutlines(t=173μs)**

As it is pictured, magnetic field inside the toroid is much higher than the outside magnetic field. Fig. 5.23 shows the variation of the magnetic field inside the toroid.

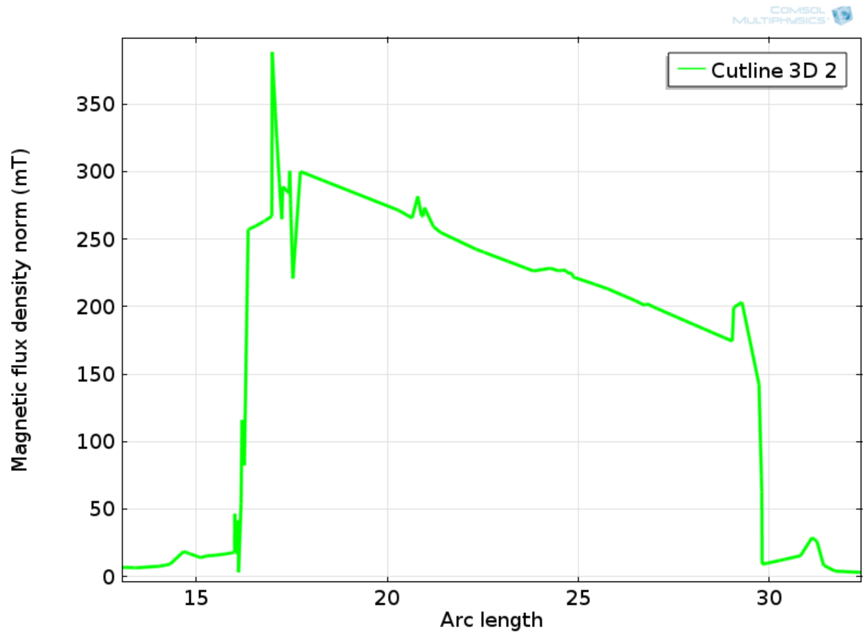


**Fig. 5.23 Magnetic field (magnetic flux density) inside the toroid(t=173µs)**

When Cutline 3D 1 passes through the toroid while the arc length is between the inner and outer radius (17cm to 30cm) a high magnetic field value is measured. As it is expected by increasing the distance from the middle point, the magnetic field is dramatically reduced which is shown in Fig. 5.24.

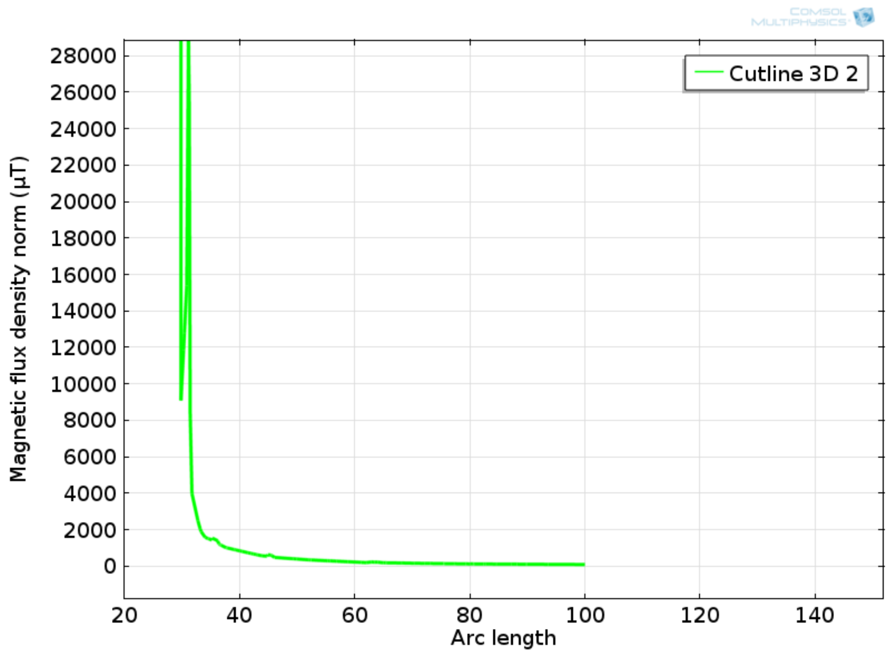


**Fig. 5.24 Magnetic field (magnetic flux density) outside the toroid(t=173µs)**

Magnetic field on the cutline 3D 2 is gradually decreased which is shown in Fig. 5.25.

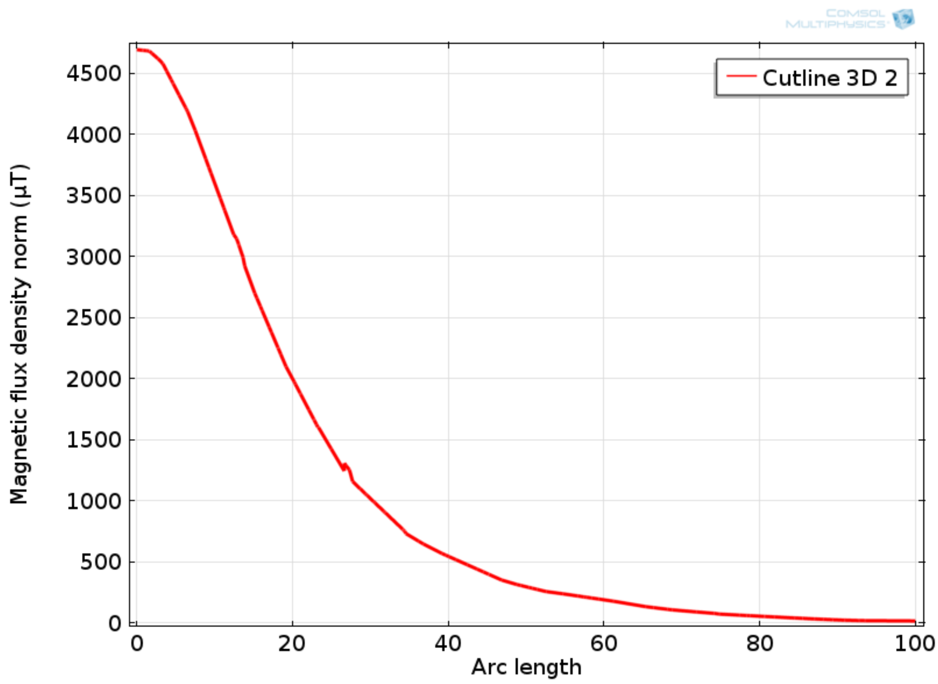


**Fig. 5.25 Magnetic field (magnetic flux density) on cutline3D 2**

Fig. 5.26 shows that there is a slightly small difference between the magnetic flux density value of Cutline 3D 1 and Cutline 3D 2, where the points are considered outside the toroid.

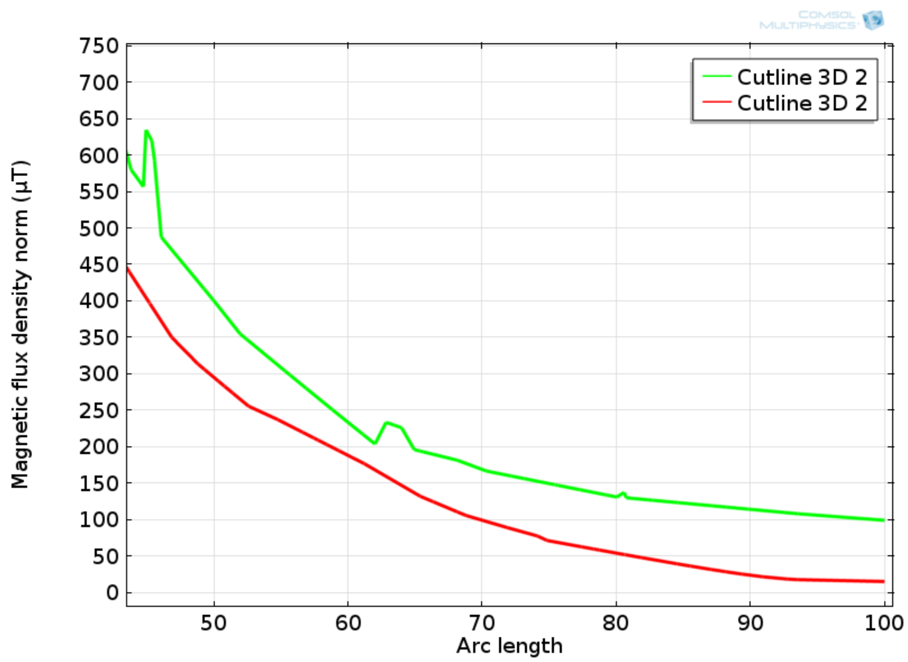


**Fig. 5.26 Magnetic field (magnetic flux density) outside the toroid(t=173µs)**

Outside magnetic field is a point of interest in this thesis. Fig. 5.27and Fig. 5.28 show Cutline 3D 3 and Cutline 3D 4 which are sketched in order to estimate the outside maximum magnetic field value, while the maximum current is applied to the inductor.

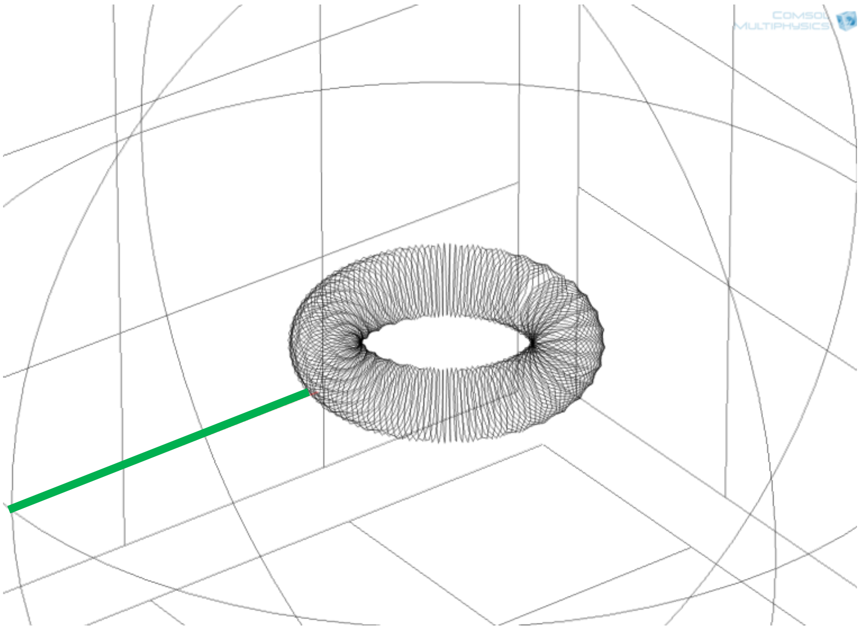


**Fig. 5.27 Cutline 3D 3**

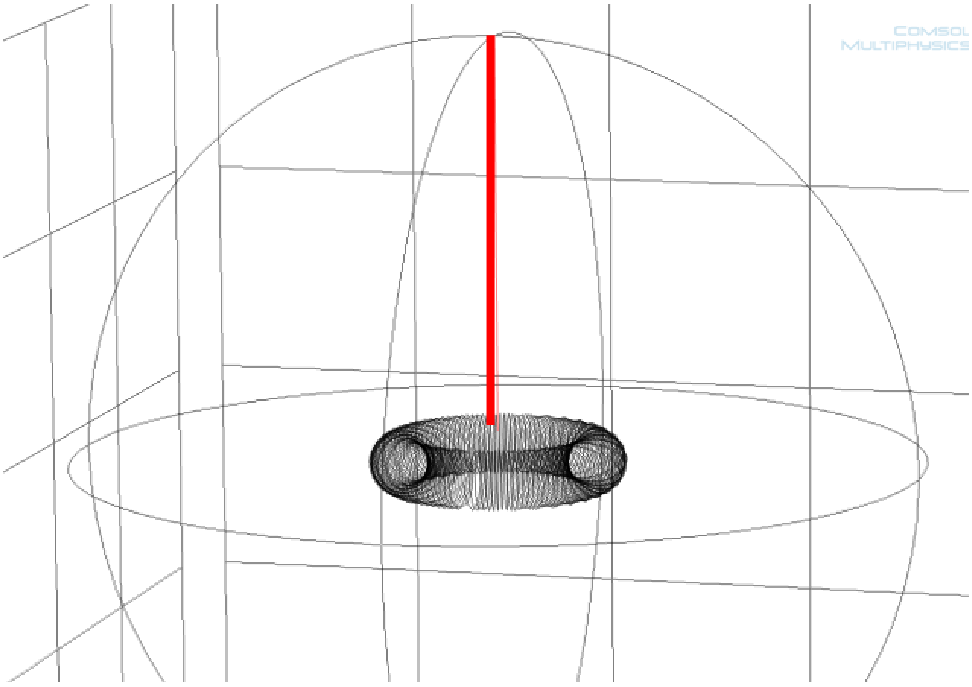


**Fig. 5.28 Cutline 3D 4**

Cutline 3D 3 is drawn from the outer part of the inductor attached to the winding while Cutline 3D 4 is drawn from the middle point of the plane attached to the top side of the inductor.

Table 7 shows the maximum magnetic field values on Cutline 3D 3 and Cutline 3D 4 at different points while the highest current(1.8 KA) is applied to the toroid.

**Table 7 Magnetic flux density around the toroidal inductor**

| *Length (cm)* | *5* | *10* | *15* | *20* | *25* | *30* | *35* | *40* | *45* | *50* | *55* | *60* | *65* | *70* |
|---|---|---|---|---|---|---|---|---|---|---|---|---|---|---|
| $B_{Cutline3D\,3}$ *(mT)* | ***1.463*** | ***0.850*** | ***0.632*** | ***0.400*** | ***0.308*** | ***0.233*** | ***0.196*** | ***0.168*** | ***0.149*** | ***0.131*** | ***0.122*** | ***0.114*** | ***0.105*** | ***0.099*** |
| $B_{Cutline3D\,4}$ *(mT)* | ***3.257*** | ***2.423*** | ***1.756*** | ***1.277*** | ***0.897*** | ***0.638*** | ***0.488*** | ***0.349*** | ***0.264*** | ***0.216*** | ***0.158*** | ***0.119*** | ***0.088*** | ***0.064*** |

As expected, according to the values, the gradually decrease of magnetic field is concluded.

## 5.3 Comparison of the cylindrical and the toroidal inductors

In order to have a better comprehension of the inductors geometries, both inductors are shown in the same photo, which is shown in Fig. 5.29.

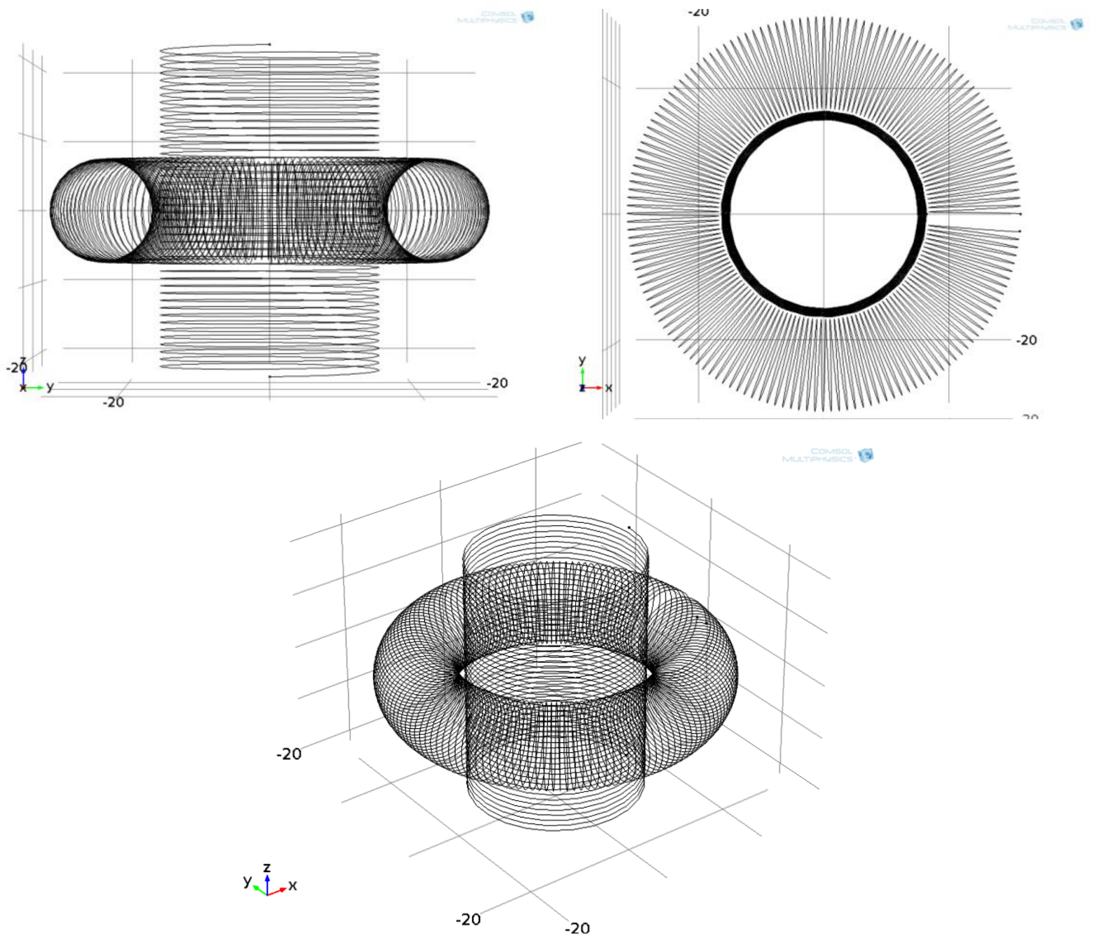


**Fig. 5.29 The cylindrical and the toroidal inductors**

As it is clearly seen, it is tried to model two inductors with possibly the same size, since the comparison is supposed to be made on the magnetic field of the inductors while the other values are kept the same.

In order to compare the magnetic field produced by the cylindrical inductor to the one produced by toroidal inductor, the aforementioned values in Table 5 and Table 7 are compared in Table 8.

**Table 8 Magnetic flux density comparison of the cylindrical inductor and the designed toroidal inductor**

| | ***Distance from the inductor(cm)*** | ***Cylindrical inductor*** | | ***Toroidal inductor*** | |
|---|---|---|---|---|---|
| | | ***Cutline3D 3*** | ***Cutline3D 4*** | ***Cutline3D 3*** | ***Cutline3D 4*** |
| *Magnetic field(mT)* | *5* | *21.308* | *67.901* | *1.463* | *3.257* |
| | *10* | *15.999* | *42.798* | *0.850* | *2.423* |
| | *15* | *12.154* | *28.886* | *0.632* | *1.756* |
| | *20* | *9.377* | *18.248* | *0.400* | *1.277* |
| | *25* | *6.764* | *11.302* | *0.308* | *0.897* |
| | *30* | *5.755* | *7.837* | *0.233* | *0.638* |
| | *35* | *4.413* | *5.598* | *0.196* | *0.488* |
| | *40* | *3.432* | *3.954* | *0.168* | *0.349* |
| | *45* | *3.131* | *2.827* | *0.149* | *0.264* |
| | *50* | *2.698* | *1.007* | *0.131* | *0.216* |
| | *55* | *2.437* | *4.410* | *0.122* | *0.158* |
| | *60* | *2.163* | *1.015* | *0.114* | *0.119* |
| | *65* | *1.898* | *0.669* | *0.105* | *0.088* |
| | *70* | *1.819* | *0.304* | *0.099* | *0.064* |

From the above it follows that the magnetic field outside the toroidal inductor is much less than of the one in the cylindrical inductor. Notice that these values are taken at t=173µs when the highest current value (1.8kA) is applied to the inductors.

# 6 Inductor Manufacturing

According to the design criteria, the toroidal inductor is made. Plywood sheet is chosen for the toroid core. Table 9 and Fig. 6.1 show the geometry of the plywood rings which play the role as the stand for the winding as well as the inductor core.

**Table 9 Plywood rings geometry**

| *a(mm)* | *b(mm)* | *h(mm)* | *Quantity* |
|---|---|---|---|
| *600±1* | *340±1* | *10±1* | *3* |
| *596±1* | *340±1* | *10±1* | *3* |
| *576±1* | *360±1* | *10±1* | *3* |
| *530±1* | *410±1* | *10±1* | *3* |

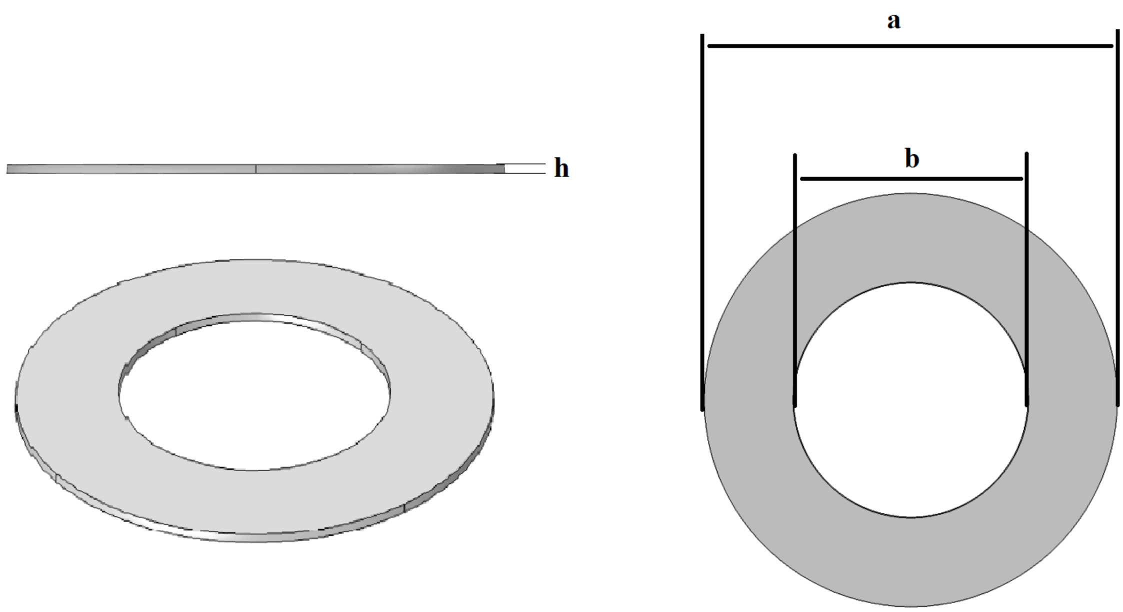


**Fig. 6.1 Plywood ring as the toroid core**

The inner radius is 17cm and the outer radius is 30cm. To avoid using several plates and in order to provide a simpler and lighter toroid, spacers are located between the rings. The rings and spacers are glued together to make the toroidal core. Fig. 6.2 shows the donut shape core as well as nuts and rod.

**Fig. 6.2 Toroidal core and fiber glass nuts and rod**

Four threaded rods made of Fiber-reinforced plastic (FRP) which are fastened by the FRP nuts play legs role for the toroid. In order to fix the winding on the toroid, teeth-like seat are made on the circumference of the toroid which is shown in Fig. 6.3.


**Fig. 6.3 Teeth-like cable seats on the circumference of the toroid**

The conductor is chosen according to the current and voltage applied to the inductor. RADOX 155 FH, 10mm$^2$ single core cable is selected [11][12][13]. Table 10shows the properties of the cable.

**Table 10 Winding cable properties**

| | |
|---|---|
| ***Cross-section*** | *10 mm²* |
| ***Voltage rating (V)*** | *600/1000* |
| ***Test voltage (V)*** | *3500* |
| ***Number of conductors*** | *1* |
| ***Conductor class*** | *IEC 60228 Class 5* |
| ***Insulation*** | *RADOX 155* |
| ***Conductor resistance*** | *1.95Ω/km* |

To avoid parasitic capacitance in multi-layers configuration due to the high voltage difference different between the layers, and also to manufacture a homogenous inductor a single layer winding is chosen which provides a single inductor value. In this case the number turns is 156 and the cable length is 70m which produces a series resistance of 136mΩ. Since there is a high voltage different between the first couple of turns and the last couple of turns of the winding, it needs to isolate them by the isolation film. Fig. 6.4 shows the Mylar film isolation.

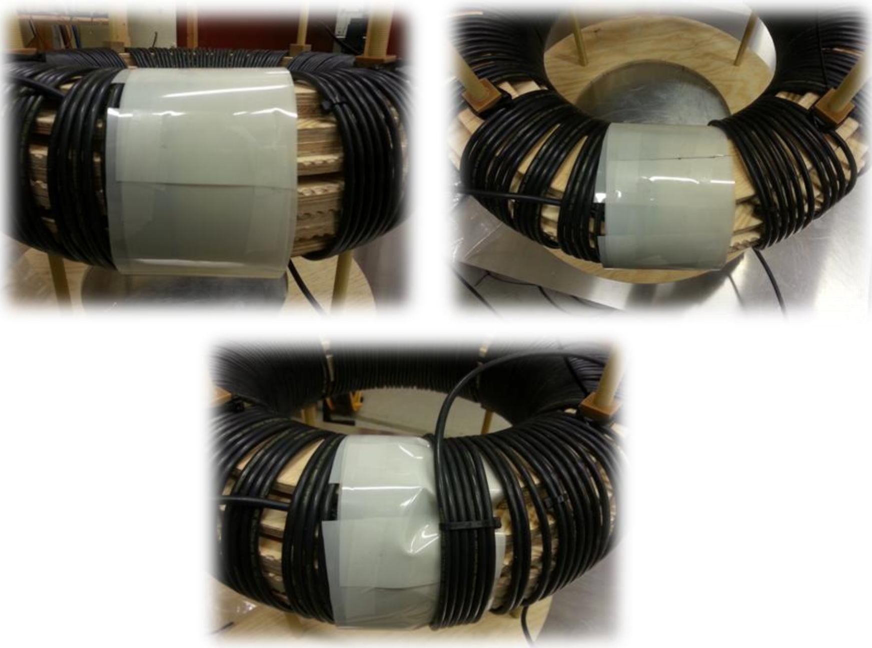

**Fig. 6.4 Mylar film isolation**

The voltage withstand of a Mylar film is a couple of 10 kilo volts. There is also a voltage difference between two adjacent turns but it is small and negligible.

A Fiberglass plate provides a robust nonconductive stand for the cable terminals and the connections which is shown in Fig. 6.5.

**Fig. 6.5 Fiberglass plate as the connection stand**

Eventually the toroid is taped with self-vulcanizing tape which is shown in Fig. 6.6.


**Fig. 6.6 Vulcanizing tape**

The material is Polyisobutylene and the dielectric strength is 35kV/mm while the temperature limit is -40°C/+90°C. Further properties are found in the appendix.

Fig. 6.7 shows the top and front view of the manufactured toroidal inductor.

**Fig. 6.7 The manufactured toroidal inductor**

At the moment of writing this report, so far, the highest current level and voltage are 2000A and 3600V, respectively. The electrical and magnetic characteristics of this inductor are presented in the next chapter.

# 7 Characteristic measurement of the toroid

## 7.1 Inductance

The RLC measurement is made on the toroid. Fig. 7.1 shows the measurement instrument.

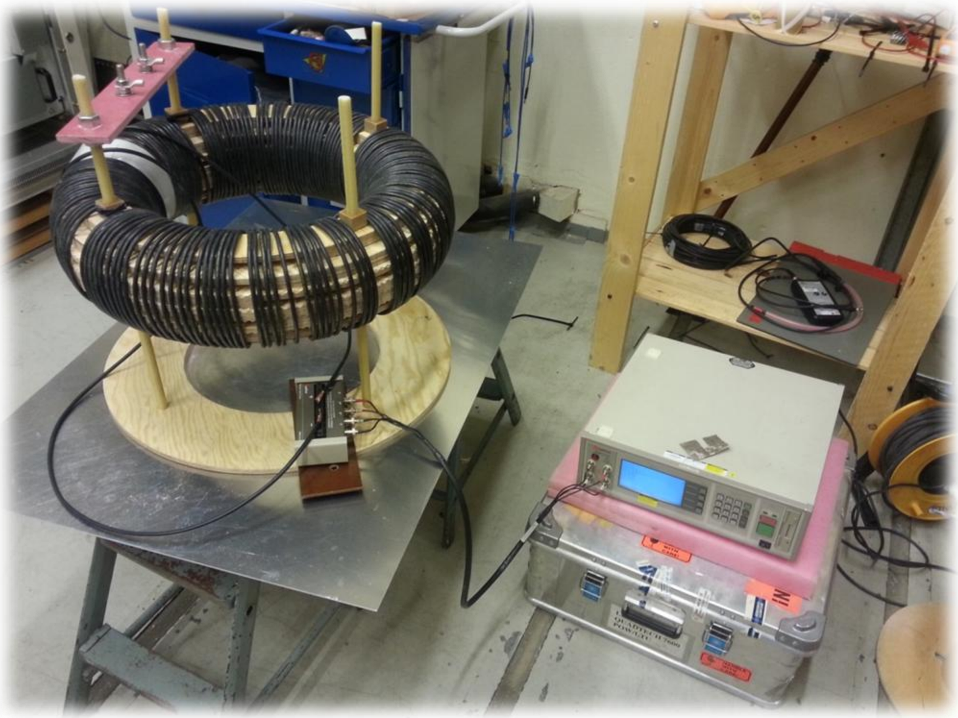

**Fig. 7.1 The toroid RLC measurement**

The inductance is calculated by using the LC circuit equation,

$$L = \frac{1}{C.(2\pi f)^2} \tag{7.1}$$

As it is shown the inductance value depends on the frequency. In this measurement a wide range of frequency is chosen to have a precise result.

Simply, the RLC meter, measures the inductance by calculating the phase angle between the voltage and the current in the toroid. Fig. 7.2 shows the result of the measurement.

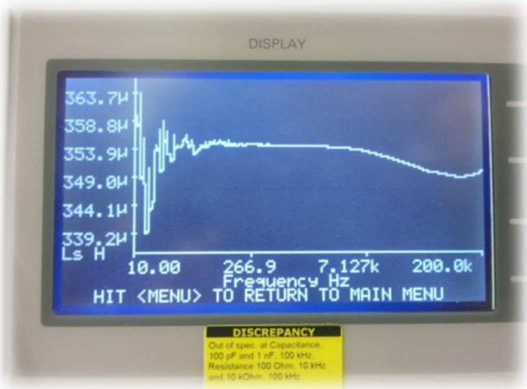


**Fig. 7.2 Inductance measurement curve on the RLC meter**

As it is seen, a wide range of frequency is chosen (10Hz to 200kHz) to estimate the inductance value. The measured inductance is about 355µH while the theoretically calculated inductance is 359µH.

## 7.2 Resistance

The conductor resistance of the cable used for the inductor is 1.95Ω/km and the measured series resistance of the inductor is 0,136Ω.

## 7.3 Magnetic field

According to Amperes' law, magnetic field inside a toroid is calculated by considering that the magnetic field is concentric with the toroid axis while the current is enclosed by N loops,

$$\oint B.dl = \mu_o I_{enclosed} \tag{7.2}$$

$$B_{Center}.2\pi r = \mu_o NI \tag{7.3}$$

Then the magnetic field "inside" the toroid is defined

$$B_{Center} = \frac{\mu_o NI}{2\pi r} \tag{7.4}$$

To measure the magnetic field spread by the inductors, a coil of wire is located in different positions. Current applied to the toroid induces the voltage in the coil. Measuring the induced voltage yields the magnetic field outside the inductors.

In our case a current pulse applied to the inductors. A quick change induces more emf than a gradual change of magnetic flux which is summarized by faradays' law,

$$e = -N\frac{d\varphi}{dt} \tag{7.5}$$

when the negative sign shows the induced electromotive force (emf) is opposing to any changes in the magnetic flux which is explained in Lenz law.

$e$: Induced electromotive force

$N$: Number of winding turns

$\varphi$ : Magnetic flux in a loop

$$\varphi = B.A.\cos\theta \tag{7.6}$$

When

$A$: Area of the coil of wire

$B$: Magnetic field of toroid

$Cos\ \theta$ : The angle between magnetic field $B$ and vector $A$(perpendicular to the plane of the coil of wire)

$\varphi$: Magnetic flux which is a measure to show the number of magnetic field lines passing through the area A

Substituting $\varphi$ in (7.5), the magnetic field outside the toroid is yield

$$\frac{dB}{dt} = \frac{e}{NA\cos\theta} \tag{7.7}$$

$$B = \int_{t_0}^{t_1} \frac{e}{NA\cos\theta}\,dt \tag{7.8}$$

In order to capture the magnetic field spreading, a circular loop is made. It is shown in Fig. 7.3, the circumference of the ring is taped by a copper tape.

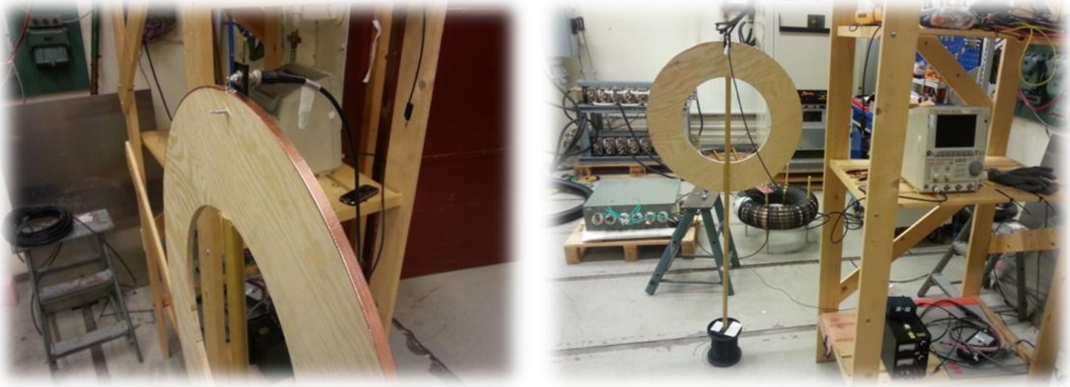

**Fig. 7.3 The circular loop to capture and measure the magnetic field spreading**

A quasi single pulse test circuit is set up in order to measure the magnetic field. The circuit and the measurement devices are shown in Fig. 7.4.

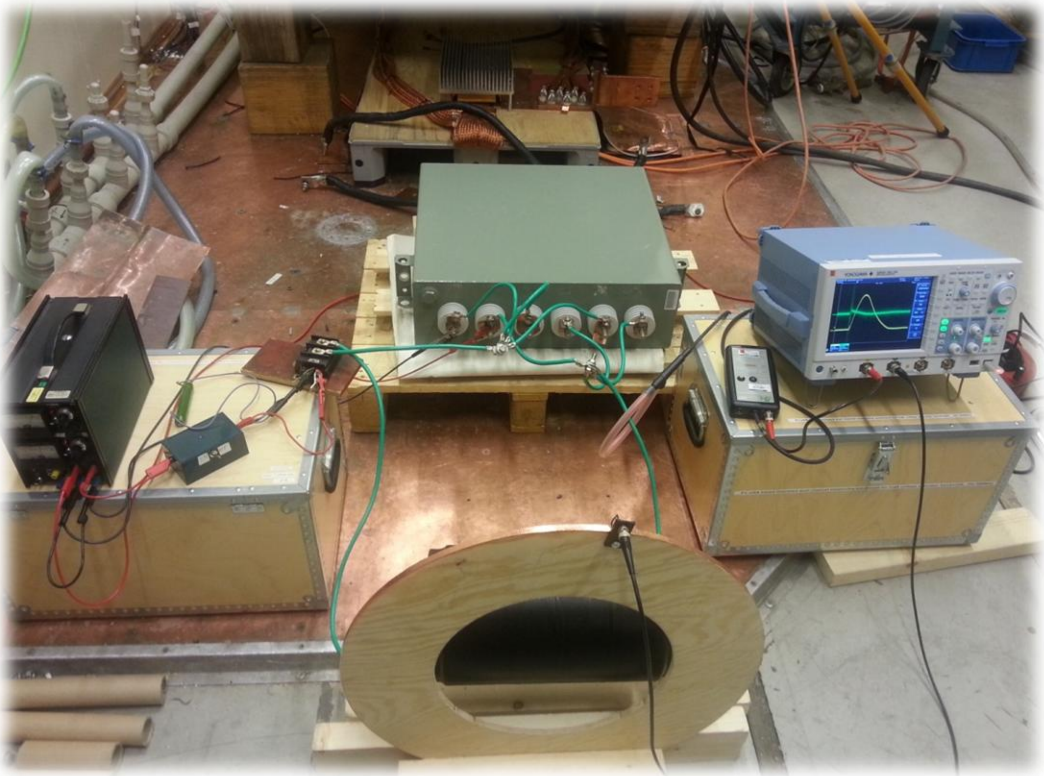

**Fig. 7.4 Test circuit set for magnetic field measurement**

The supply unit charges the capacitor and the switch is to trigger the gate and discharge the capacitor. The circular loop captures the magnetic field produces by the inductor while the current passes through it. The oscilloscope monitors the inductor current waveform and the induced voltage in the circular loop. Note that the current applied to the inductor is much lower than the actual application. In this study, two inductors are "compared". In the following waveform, the green curve represents the current passing through the inductor and yellow curves shows the induced voltage in the circular loop.

### 7.3.1 Cylindrical inductor magnetic field measurement

The circular loop is located in different positions with different angle to the inductor.

*Front position*

Fig. 7.5 shows the waveforms pictured on the oscilloscope and the position of the circular loop while it is located in position "Front, A".

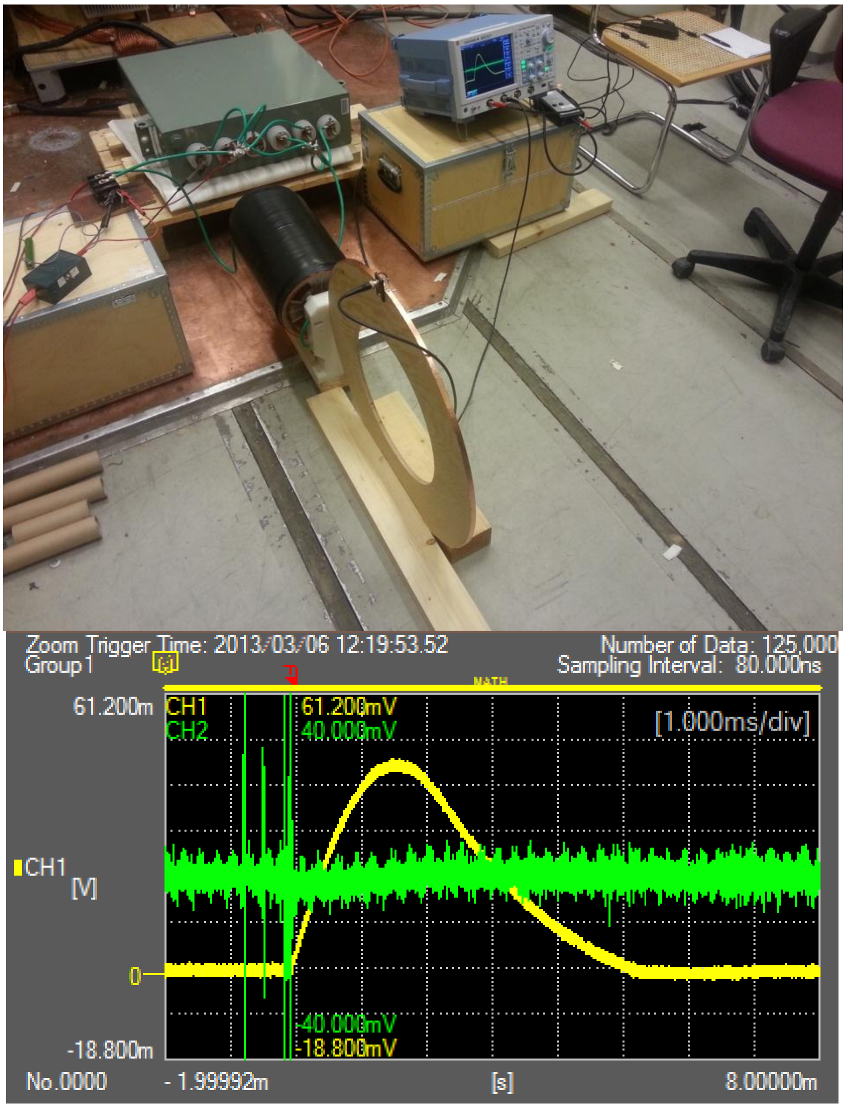


**Fig. 7.5 Measured waveforms and circular loop(position Front, A)**

The yellow waveform shows the inductor current and the green waveform pictures the induced voltage in the circular loop. Since number of magnetic field lines is almost equal in both side of the circular loop with opposite directions, the summation of the magnetic field is around zero and the induced voltage is not significant, however the circular loop is attached to the inductor.

If the circular loop is rotated by 90 degrees, the induced voltage will dramatically increase which is shown in Fig. 7.6.

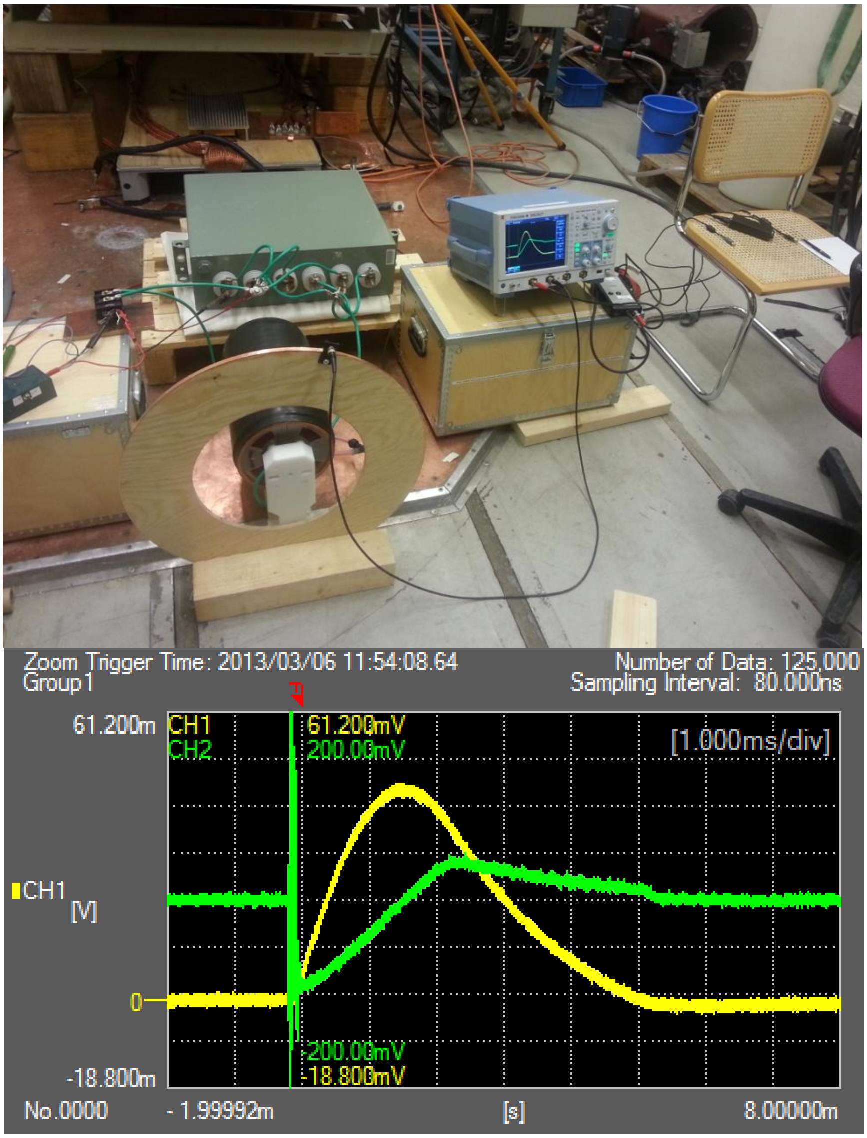


**Fig. 7.6 Measured waveforms and loop position which is attached to the inductor(position Front, B)**

By increasing the distance of the circular loop to the inductor, the induced voltage decreases. Fig. 7.7 shows the measured waveform while the circular loop is located in different positions away from the inductor while the position is shown in Fig. 7.8.

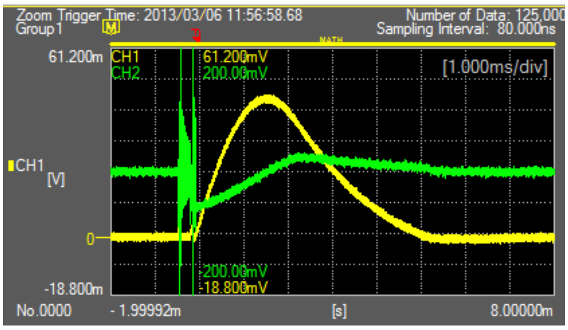


**10cm**

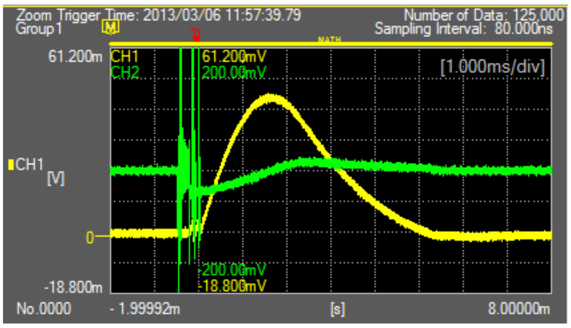


**20cm**

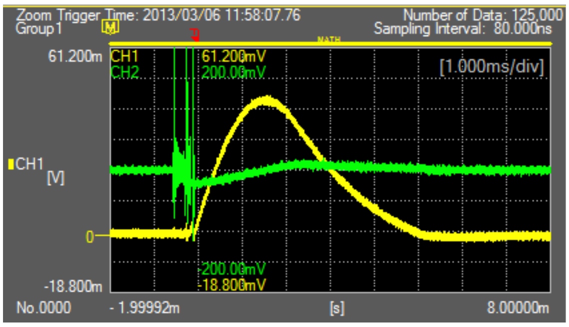


**30cm**

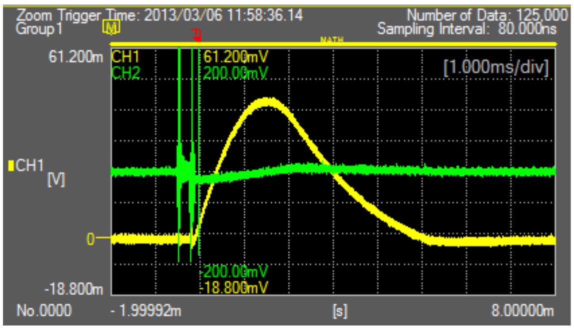


**40cm**

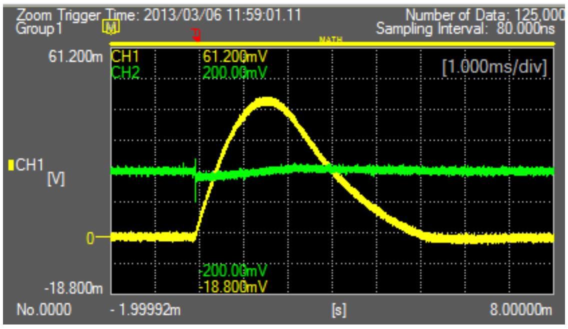


**50cm**

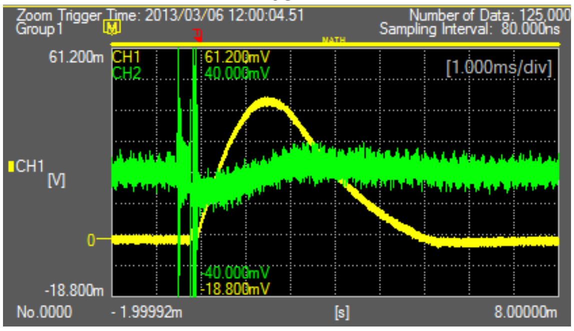


**60cm**

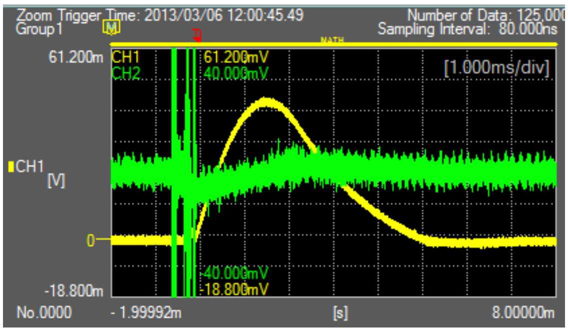


**70cm**

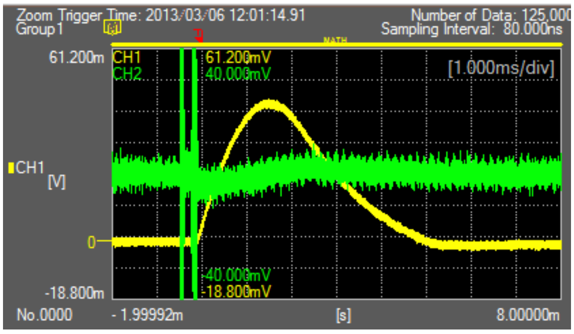


**80cm**

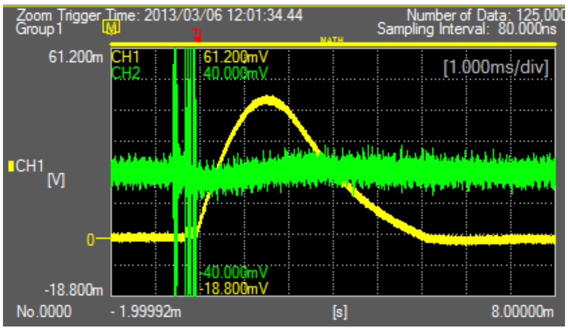


**90cm**

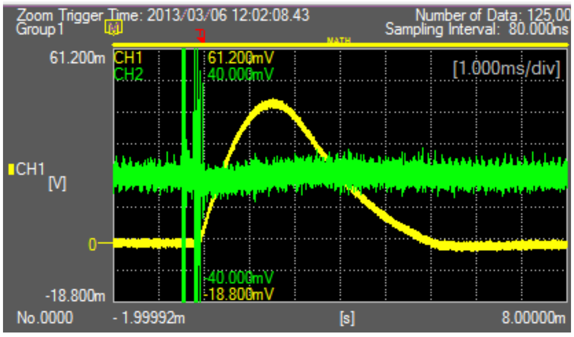


**100cm**

**Fig. 7.7 Waveforms when the loop is located in different position away from the inductor(position Front, B)**

**Fig. 7.8 Circular loop is located 100cm away from the inductor(position Front, B)**

According to the waveforms by moving the circular loop away from the inductor, magnetic field is reducing, which is expected.

*Side position*

Fig. 7.9 shows the waveform and the position of the attached loop while the circular loop is located in “Side position”.

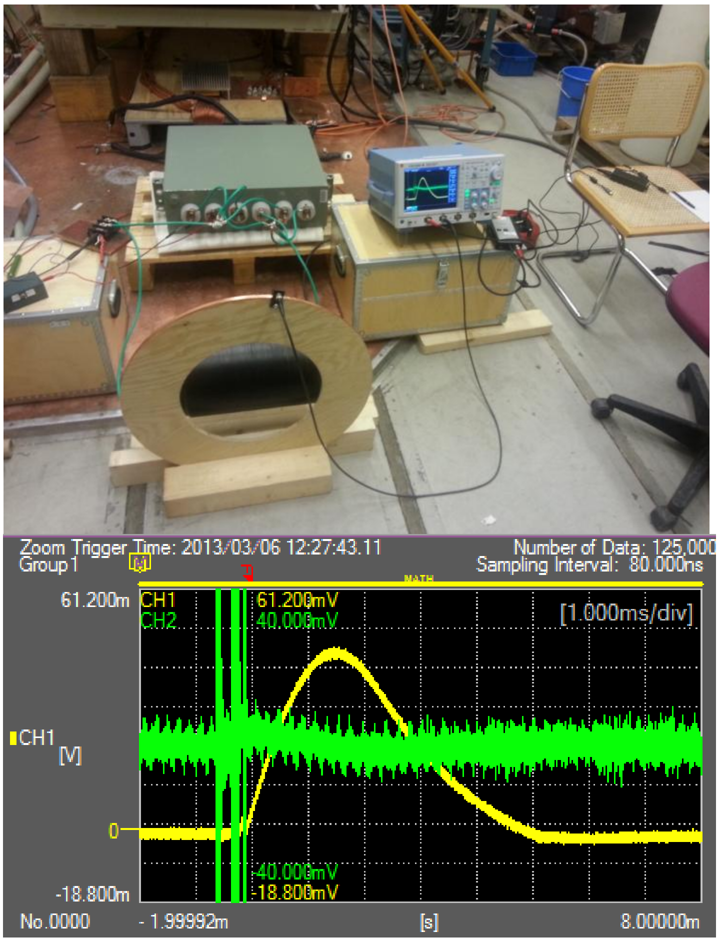


**Fig. 7.9 Circular loop attached to the inductor(position Side, A)**

In this position, although the circular loop is attached to the inductor, the induced voltage is so low. And it is due to the fact that the magnetic field lines are in parallel with the loop and they are not captured.

Changing the circular loop angle shows a significant value of induced voltage. Fig. 7.10 shows the position of the circular loop and the waveforms.

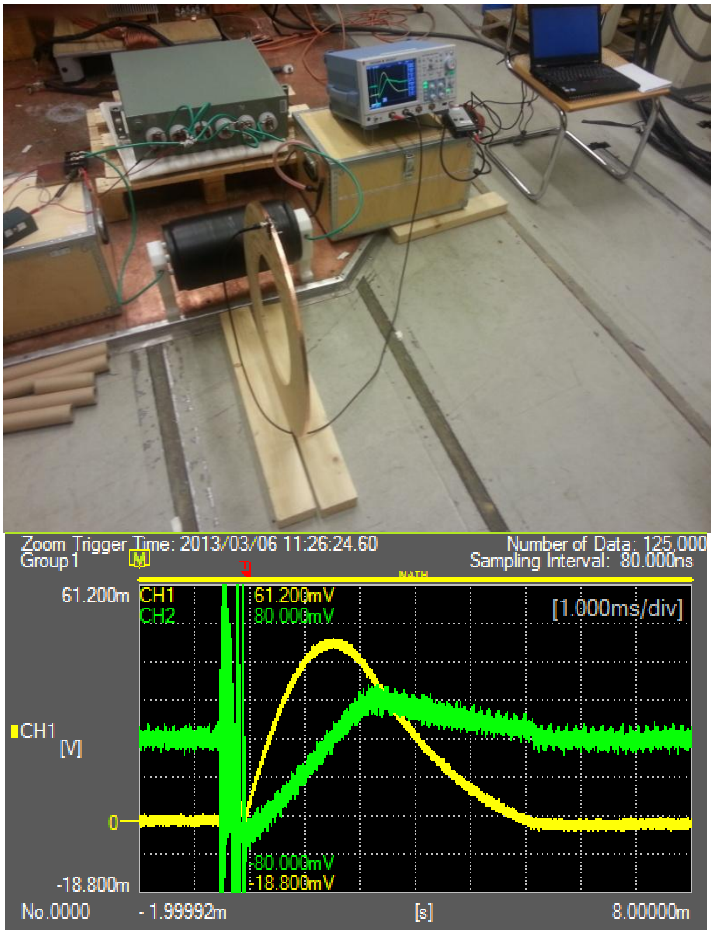


**Fig. 7.10 Circular loop attached to the inductor(position Side, B)**

This position shows the highest value of induced voltage (magnetic field). The magnetic field lines are perpendicular to the circular loop, and they are all heading to the same direction.

By the circular loop away from the inductor, the magnetic field spread decrease. The measured waveforms are shown in Fig. 7.11 while the position is observed in Fig. 7.12.

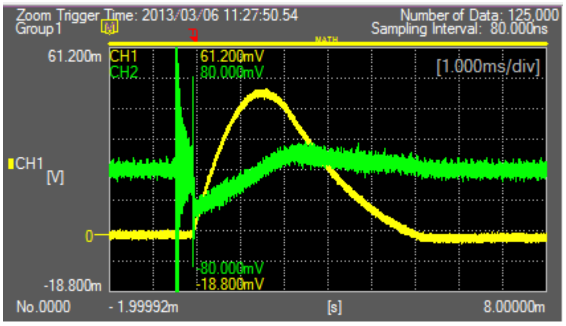


**10cm**

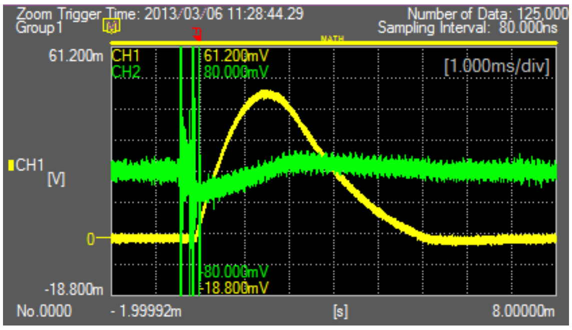


**20cm**

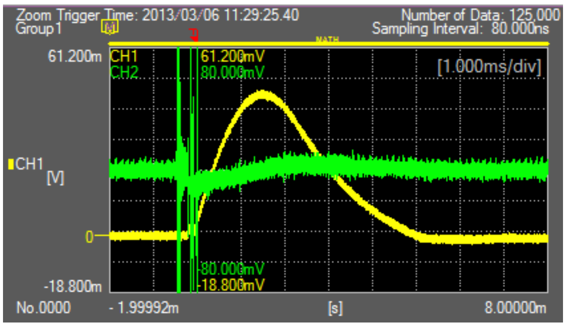


**30cm**

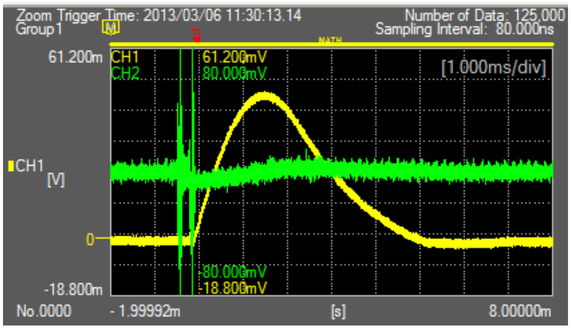


**40cm**

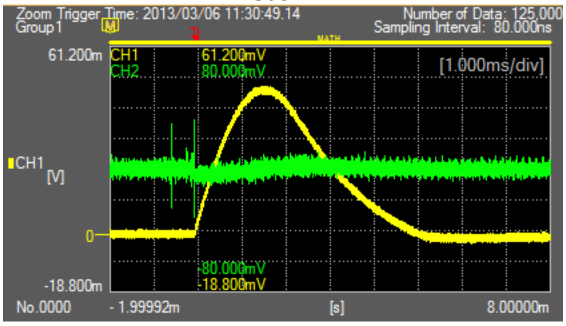


**50cm**

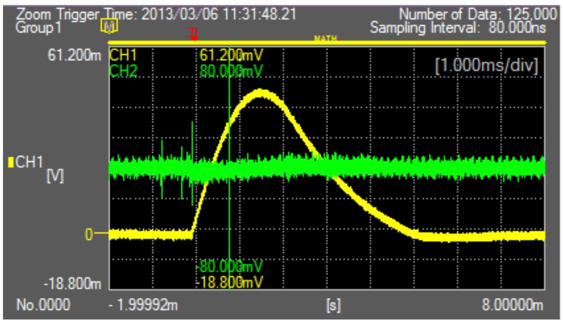


**60cm**

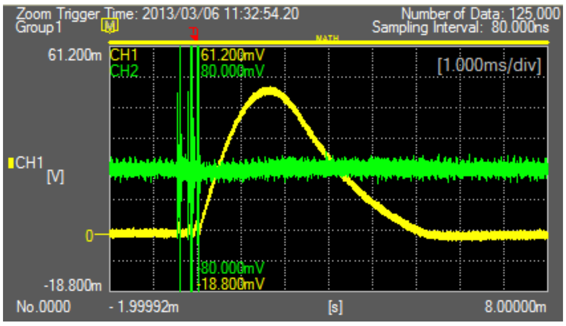


**70cm**

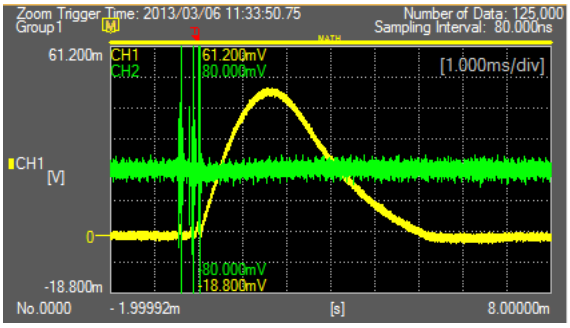


**80cm**

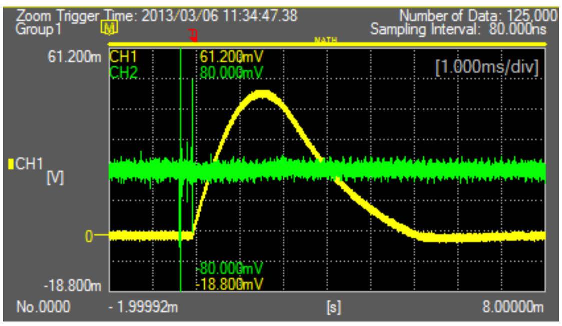


**90cm**

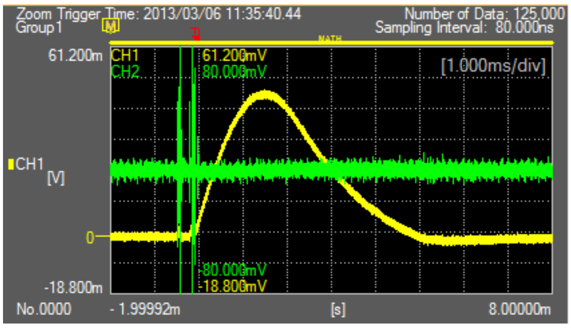


**100cm**

**Fig. 7.11 Waveforms while the loop is located in different position away from the inductor(position Side, B)**

**Fig. 7.12 Circular loop is located 100cm away from the inductor(position Side, B)**

According to the waveforms, by increasing the distance between the circular loop and the inductor, the magnetic field reduces dramatically. At 100cm away from the inductor, almost no magnetic field can be measured.

### 7.3.2 Toroidal inductor magnetic field measurement

The same current level as applied to the cylindrical inductor is applied to the toroidal inductor to compare the magnetic spread. Theoretically, it is known that the magnetic field of a toroidal inductor is accumulated inside the inductor. But practically, there is still some magnetic field spread outside a toroidal inductor. In order to measure the magnetic field spread of the toroidal inductor, the circular loop is located in different positions. Fig. 7.13 shows the waveforms and the position of the circular loop attached to the inductor.

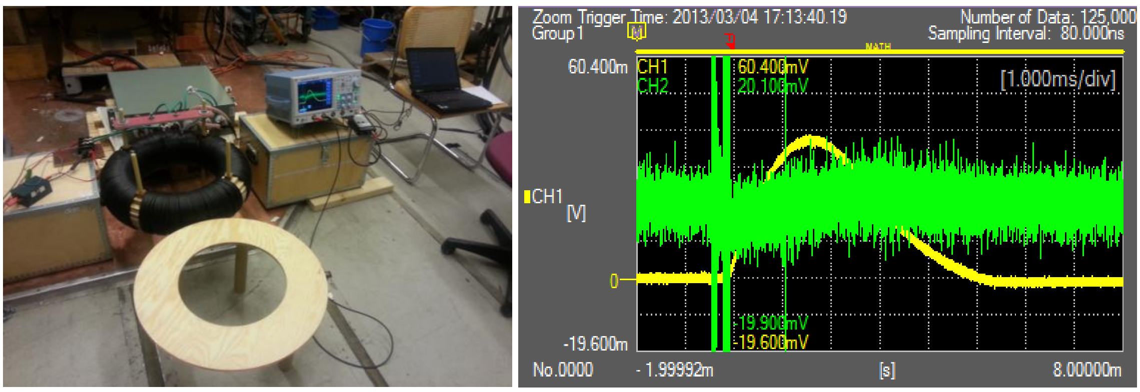


**Fig. 7.13 Measured waveforms while the circular loop is attached to the side corner of the inductor(position A)**

As it is seen, there is slightly low induced voltage measured which declares the low magnetic field spread of the inductor. At the moment of switching, there are some oscillations which are cause by glitching of the switch. The circular loop is moved on the surface of the inductor to measure the induced voltage. Fig. 7.14 shows the position of the circular loop and measured waveforms.

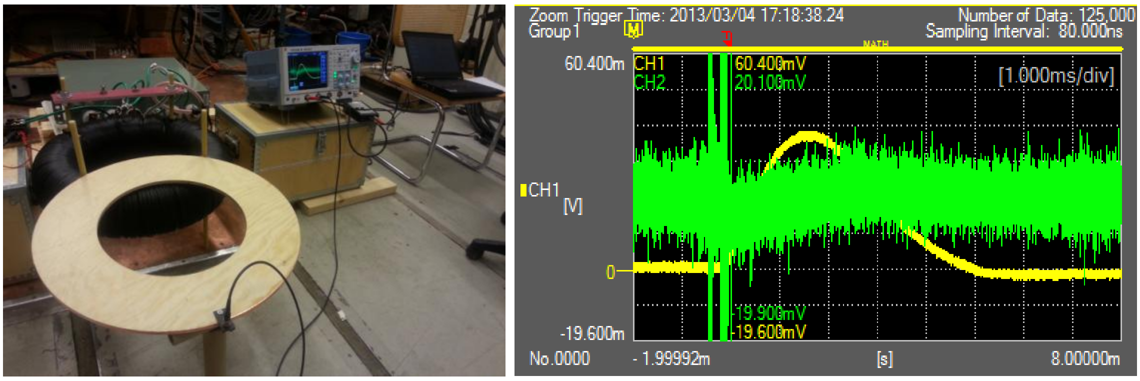


**Fig. 7.14 Circular position and measured waveforms(position B)**

The measured induced voltage is slightly higher than the attached circular loop, but in comparison with cylindrical inductor, the induced voltage is negligible. The circular loop is located above the inductor, and the results are pictured in Fig. 7.15.

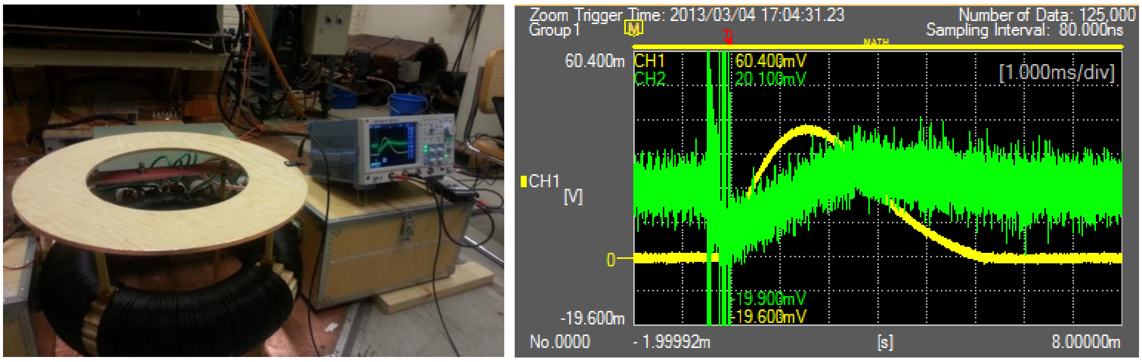


**Fig. 7.15 Circular position and measured waveforms(position C)**

The induced voltage in this case increases, but it is still so low in comparison with the cylindrical inductor. Changing the angle of the circular loop has no effect on magnetic field capturing, since the value is so low. Fig. 7.16 shows the circular loop and the measured waveform while the circular loop is in vertical position.

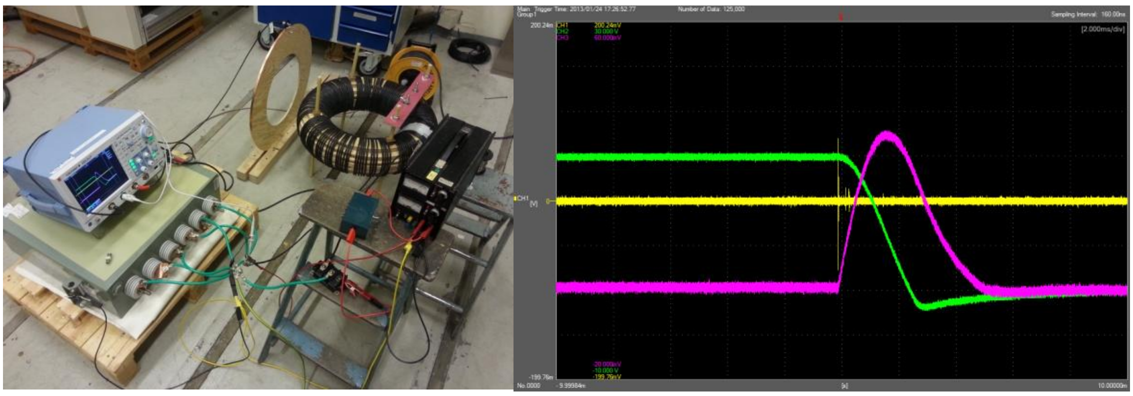

**Fig. 7.16 Circular loop position and measured waveforms(position D)**

The Magenta waveform shows current through the inductor, the green waveform shows the voltage over the capacitor and the yellow waveform shows the induced voltage in the circular loop. As it is seen the value of the induced voltage is so low to be measured while glitching of the switch is appeared on the screen.

### 7.3.3 Magnetic field comparison

So far, the induced voltage is measured. According to the measured induced voltage and (7.8), magnetic field spread of the inductors is calculated. Table 11 and shows the calculated magnetic field spread of both cylindrical and toroidal inductors.

**Table 11 Calculated magnetic flux density**

| Distance (cm) | Magnetic field spread(μT) | | | | | |
|---|---|---|---|---|---|---|
| | Cylindrical Inductor Position Front | | Cylindrical Inductor Position Side | | Toroidal Inductor | Position |
| | A | B | A | B | | |
| Attached | 5.12 | 307 | 11.25 | 184.30 | **6.69** | **A** |
| 10 | ---- | 174.20 | ---- | 76.07 | **8.77** | **B** |
| 20 | ---- | 120.40 | ---- | 45.37 | **21.01** | **C** |
| 30 | ---- | 74.82 | ---- | 29.08 | **0.28** | **D** |
| 40 | ---- | 43.40 | ---- | 18.81 | | |
| 50 | ---- | 29.20 | ---- | 11.50 | | |
| 60 | ---- | 22.07 | ---- | 8.23 | | |
| 70 | ---- | 17.42 | ---- | 6.30 | | |
| 80 | ---- | 11.70 | ---- | 4.56 | | |
| 90 | ---- | 08.95 | ---- | 3.76 | | |
| 100 | ---- | 06.72 | ---- | 2.95 | | |

It is clearly seen by increasing the distance away from the inductor the magnetic flux density reduces dramatically. According to table, the magnetic field spread of the toroidal inductor is much lower than the one of cylindrical inductor. Note that this comparison has been made while the same current level (40A) applied to the inductors. Although the toroidal inductor has higher inductance value than the cylindrical inductor (355μH vs. 270μH), the magnetic field spread is much lower. Fig. 7.17 pictured the variation of the magnetic field by distance between the circular loop and the cylindrical inductor.

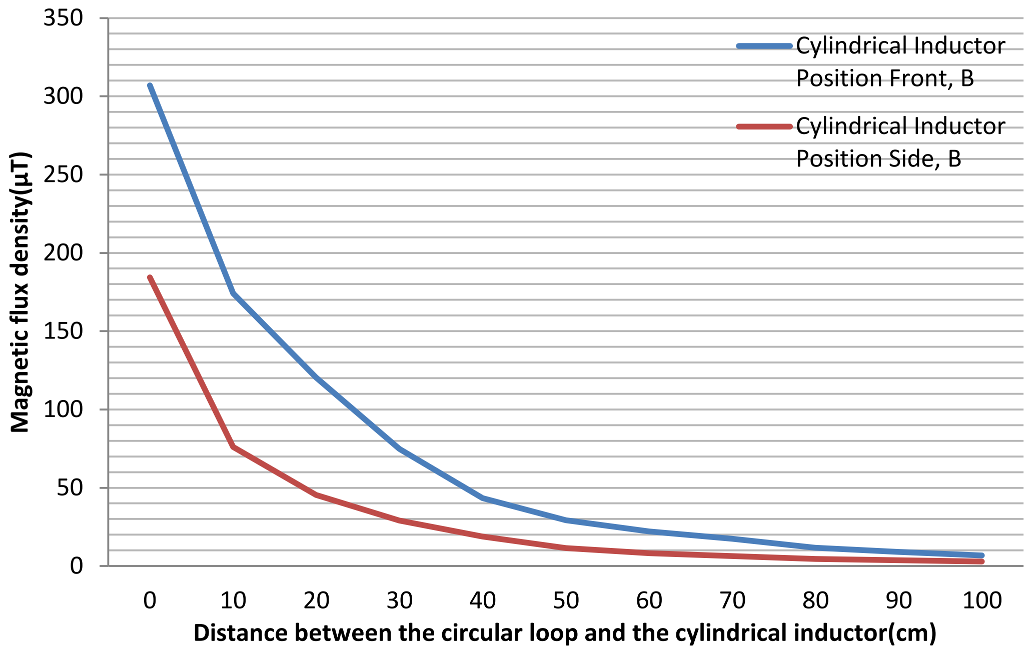


**Fig. 7.17 Magnetic flux density variation by circular loop distance from the cylindrical inductor**

Considering position "Front, B", when the circular loop is attached to the cylindrical inductor, highest value of magnetic field is captured. Moving the circular loop 10cm away from the inductor, the magnetic field reduces by 43%, likewise when the distance increases to 20cm, the magnetic field reduction is 61%. Fig. 7.18 shows the magnetic flux density at 10cm away from inductors in different positions.

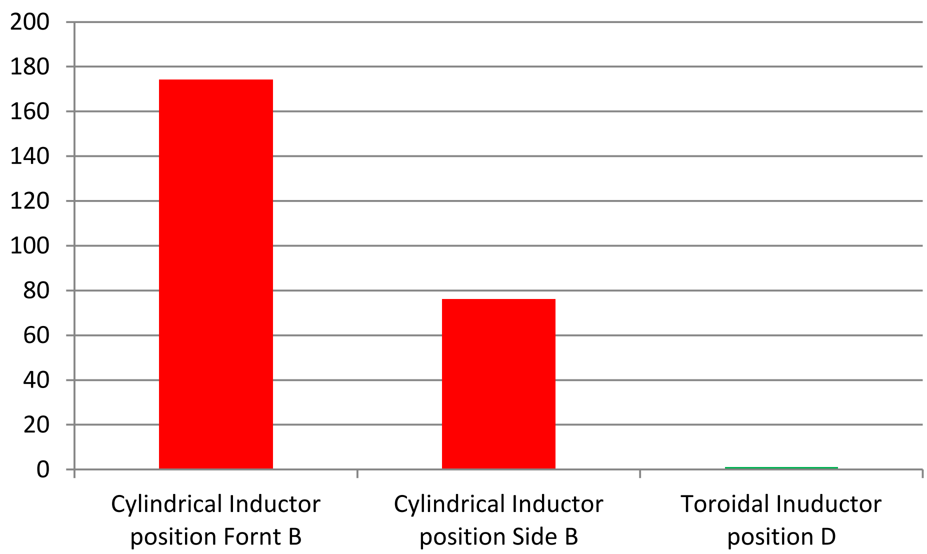


**Fig. 7.18 Magnetic flux density(µT)at 10cm away from the inductors**

Magnetic field in toroidal inductor is considerably reduced, although the inductance of the toroidal inductor is higher than the cylindrical inductor.

# 8 Conclusion

In this thesis a new inductor has been designed and manufactured for the single pulse test circuit with the purpose of magnetic field disturbance reduction. A cylindrical inductor and a toroidal inductor are simulated in COMSOL Multiphysics® in order to investigate and compare the magnetic field spread in both inductor types. According to the comparison made in COMSOL Multiphysics®, it is observed that the magnetic field of the toroidal inductor is much less than the one of the cylindrical inductor for the same current (1.8kA) and inductance value (270µH). The magnetic field of the toroidal inductor shows a dramatic reduction compared to the magnetic field of the cylindrical inductor. At a horizontal distance of 10cm from the inductors, the magnetic field is reduced from 42.798µT in the cylindrical inductor case to 2.423µT in the toroidal inductor case; likewise at a vertical distance of 10cm from the inductors, the magnetic field is reduced from 15.999µT in the cylindrical inductor case to 0.850µT in the toroidal inductor case.

A Quasi single pulse test circuit is set up in order to measure the magnetic field disturbances. The pulse test performance and the magnetic field calculation showed a good agreement to the desired results. The magnetic field results show a dramatic reduction of the magnetic field spread in the toroidal inductor compared with the cylindrical inductor. At a distance of 10cm from the inductors, the magnetic flux density is reduced from 307µT in the cylindrical inductor case to 0.28µT in the toroidal inductor case. Moving the circular loop 10cm away from the cylindrical inductor, the magnetic field is reduced by 43%, likewise when the distance increases to 20cm, the magnetic field reduction is 61%. In this thesis a significant reduction of the magnetic field in the toroidal inductor compared with the cylindrical inductor is achieved.

The prototype toroidal inductor has been tested with exemplary samples and the result verified the improvement of the circuit component. At the moment of writing this report, so far, the highest current level and voltage are 2000A and 3600V, respectively.

# 9 Future work

In order to reduce the magnetic field spread by the inductor, a new inductor is designed and manufactured which provides a toroidal inductor with a new inductance value. Another approach to decrease the magnetic field is to shield the inductor. Although the magnetic field in the vicinity of the toroid is dramatically reduced in comparison with cylindrical inductor, in order to improve the magnetic field reduction, one could shield the toroidal inductor. Copper, galvanized steel and Aluminum are the most common shielding materials which are used in order to reduce the high magnetic field spread. The conductivity of this material is high not unlike the very low magnetic permeability. This attribute contributes to the magnetic field spread reduction of the toroid.

Another improvement of this work is to consider a shield wall around the lab in order to eliminate the magnetic field effect on neighbor labs and operators. The investigation of the effect of the magnetic field on operators, human body and brain also seems to be interesting and important. The International Commission on Non-Ionizing Radiation Protection (ICNIRP) [14] is a good reference to start from. According to experience a 5mm copper shield around the magnetic field source or test lab is needed if the magnetic field exceeds the standard value. The thickness variation of the shield from 2mm to 5mm is considerable. But increasing the thickness of the shield further than 5mm is not economical and also the effect is not notable. One can compare different thickness of the shield around the inductor to see the variation of the magnetic field by the variation of the shield thickness.

In lab application, according to a test object and test specifications, various inductor value are required. Since this inductor is manufactured for lab application, one other improvement of this work could be the design of a multi-value inductor with multiple outputs while comparison of voltage sharing between turns and winding layers, and also capacitive currents in two inductors is a point of interest.

Investigation of the possibility of applying a toroidal inductor as a high pass filter in large size for the power system application is also beneficial.

# 10 References


[1] [Online]. http://www.abb.com/semiconductors

[2] Ned Mohan, Tore Undeland, and William Robbins, *Power Electronics Converters, Applications, And Design*.: John Wiley, 2003.

[3] C. W. T. McLyman, *Transformer and inductor design handbook*.

[4] Leonard Crane, "Ferrite and Powder Core Materials for Power Inductors," 2009.

[5] "Magnetic properties of materials," , Ee.surrey.ac.uk. Retrieved 2011-11-08. [Online]. http://info.ee.surrey.ac.uk/Workshop/advice/coils/mu/

[6] S. Y. (Ron) Hui, andHenry Shu-Hung Chung S. C. Tang, "Coreless Planar Printed-Circuit-Board Transformers—A Fundamental Concept for Signal and Energy Transfer," *IEEE TRANSACTIONS ON POWER ELECTRONICS*, vol. 15, SEPTEMBER 2000.

[7] S. Y. (Ron) Hui, and Henry Shu-Hung Chung S. C. Tang, "Characterization of Coreless Printed Circuit Board (PCB) Transformers," *IEEE TRANSACTIONS ON POWER ELECTRONICS*, vol. 15, novemeber 2000.

[8] S. C. Tang, and Henry Shu-hung Chung S. Y. (Ron) Hui, "Some Electromagnetic Aspects of Coreless PCB Transformers," *IEEE TRANSACTIONS ON POWER ELECTRONICS*, vol. 15, JULY 2000.

[9] "B. D. Cullity and C. D. Graham (2008), Introduction to Magnetic Materials, 2nd edition, 568 pp., p.16,".

[10] COMSOL Multyphysics®. [Online]. http://www.comsol.com/company/

[11] HUBER+SUHNER. [Online]. http://www.hubersuhner.com.hk/co-hk/mozilla/hs-p-es-cab-over-abc-rx155

[12] Cable datasheet. [Online].

https://www1.elfa.se/data1/wwwroot/assets/datasheets/zzRadox155_dat_E.pdf

[13] Cable datasheet. [Online].
https://www1.elfa.se/data1/wwwroot/assets/datasheets/RX155_eng_tds.pdf

[14] International Commission on Non-Ionizing Radiation Protection. [Online].
http://www.icnirp.de/

# 11 Appendix

*The toroidal inductor cable data sheet:*

**RADOX® 155**
**Connecting leads**

**GENERAL PROPERTIES :**
Excellent high temperature, low temperature, ozone and weathering resistance,
flame retardant, soldering iron resistant, easy to strip and process, compatible to all common resins and varnishes, flexible.

**APPLICATION :**
For protected and fixed installation inside electrical equipment, especially suitable for the connection of motor windings, switchboards, magnets and transformers.

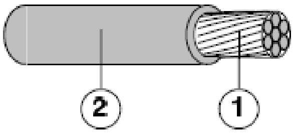


1. Conductor : Stranded tin plated copper, class 5 EN 60228
2. Insulation : RADOX 155,
   extruded irradiation crosslinked polyolefin
   Colours : diverse

PRINTING :

| | |
|---|---|
| 0.25–0.5 mm²: | HUBER+SUHNER SWITZERLAND RADOX 155 ...MM2 |
| 0.75–1 mm²: | HUBER+SUHNER SWITZERLAND RADOX 155 ...MM2 VDE-REG-NR.9331 |
| 1.5–4 mm²: | HUBER+SUHNER SWITZERLAND RADOX 155 ...MM2 VDE-REG-NR.5596 |
| ≥6 mm²: | HUBER+SUHNER SWITZERLAND [Lot No.] RADOX 155 ...MM2 VDE-REG-NR.5596 |

**TECHNICAL DATA:**

Temperature range ........................................ – 55 ... + 155 ..... °C

**Voltages for cross-section ≥ 0.75 mm²:**

Rated voltage cond.-earth ................................ $U_0$ .............. 600 V AC
Rated voltage cond.-cond. ................................ U ............... 1000 V AC
Maximum permitted operating voltage cond.-earth ................................ 720 V AC
Maximum permitted operating voltage cond.-cond. ............... $U_m$ ............. 1200 V AC
Maximum permitted operating voltage cond.-earth ............... $V_0$ .............. 900 V DC
Maximum permitted operating voltage cond.-cond. ................................ 1800 V DC
Test voltage ............................................................ 3500 V AC

**Voltages for cross-section < 0.75 mm²:**

Rated voltage cond.-earth ................................ $U_0$ .............. 450 V AC
Rated voltage cond.-cond. ................................ U ............... 750 V AC
Maximum permitted operating voltage cond.-earth ................................ 480 V AC
Maximum permitted operating voltage cond.-cond. ............... $U_m$ ............. 825 V AC
Maximum permitted operating voltage cond.-earth ............... $V_0$ .............. 620 V DC
Maximum permitted operating voltage cond.-cond. ................................ 1240 V DC
Test voltage ............................................................ 2500 V AC

Minimum bending radius ................ Outer diameter ≤ 12 mm ................ 3 x D
.................................... Outer diameter > 12 mm ................ 4 x D




HUBER+SUHNER
Wire+Cable Division
CH-8330 Pfäffikon
+41 (0)44 952 22 11
FAX +41 (0)44 952 26 40
www.hubersuhner.com


| Issue | Release | Supersedes issue | Technical Datasheet | |
|---|---|---|---|---|
| 07.10.2011 / 2031 | 2453 | G/24.08.2011 | Page 1/2 | 559 928 H (e) |

# RADOX® 155
# Connecting leads

**TABLE 1 :** Dimensions, conductor resistance, weight

| **Cross-section** EN 60228 mm² | **Conductor construction** nom. n x mmØ | **Conductor diameter** max. mm | **Outer diameter D** mm | $R_{20}$ **Conductor resistance** max. at 20°C Ω / km | **Weight** nom. kg / 100m |
|---|---|---|---|---|---|
| 0.25 | 19 x 0.13 | 0.61 | 1.45 ± 0.05 | 86.0 | 0.4 |
| 0.34 | 19 x 0.16 | 0.77 | 1.60 ± 0.10 | 53.1 | 0.5 |
| 0.5 | 19 x 0.18 | 0.90 | 1.71 ± 0.10 | 40.1 | 0.7 |
| 0.75 | 24 x 0.20 | 1.13 | 2.25 ± 0.10 | 26.7 | 1.1 |
| 1 | 32 x 0.20 | 1.28 | 2.50 ± 0.10 | 20.0 | 1.5 |
| 1.5 | 30 x 0.25 | 1.52 | 2.85 ± 0.10 | 13.7 | 1.9 |
| 2.5 | 48 x 0.25 | 2.06 | 3.50 ± 0.10 | 8.21 | 3.0 |
| 4 | 56 x 0.30 | 2.64 | 4.20 ± 0.15 | 5.09 | 4.5 |
| 6 | 84 x 0.30 | 2.98 | 5.0 ± 0.15 | 3.39 | 6.5 |
| 10 | 80 x 0.40 | 3.94 | 6.4 ± 0.15 | 1.95 | 11 |
| 16 | 119 x 0.40 | 5.4 | 7.6 ± 0.15 | 1.24 | 16.5 |
| 25 | 182 x 0.40 | 6.7 | 9.2 ± 0.2 | 0.795 | 25 |
| 35 | 266 x 0.40 | 7.9 | 10.6 ± 0.2 | 0.565 | 34.5 |
| 50 | 378 x 0.40 | 9.4 | 12.4 ± 0.25 | 0.393 | 50 |
| 70 | 348 x 0.50 | 11.5 | 14.6 ± 0.25 | 0.277 | 68 |
| 95 | 444 x 0.50 | 13.0 | 16.4 ± 0.3 | 0.210 | 89 |
| 120 | 570 x 0.50 | 15.4 | 18.5 ± 0.3 | 0.164 | 110 |
| 150 | 722 x 0.50 | 17.0 | 20.8 ± 0.3 | 0.132 | 142 |
| 185 | 874 x 0.50 | 18.5 | 22.7 ± 0.3 | 0.108 | 171 |
| 240 | 1147 x 0.50 | 21.3 | 26.1 ± 0.4 | 0.0817 | 225 |

*Vulcanizing tape properties:*

ETAB®

# PRODUKTINFORMATION

| | |
|---|---|
| **Produkt:** | Självvulkande tejp |
| **Produktnummer:** | 2050 |
| **Material:** | Polyisobutylen |
| **Tjocklek:** | 0,50 mm |
| **Färg:** | Svart, vit |
| **Draghållfasthet:** | 2,2 MPa |
| **Max töjning:** | 650 % |
| **Temp. gräns:** | -40°C/ +90°C |
| **Genomslagshållfasthet:** | 35 kV/mm |
| **Volymresistivitet:** | >$10^{13}$ Ohm\cm |

| | |
|---|---|
| **Egenskaper:** | Självvulkande tejp av PIB (polyisobutylen). Sammansmälter till homogen massa inom några timmar. Bör skyddas av mjuk plasttejp alternativt eltejp vid risk för nötning eller påverkan av UV-ljus och fuktigt väder. Viss UV-tålighet. Med skyddsliner. |
| **Användningsområden:** | För vattentät skarvning av kablar och skydd mot korrosion på rör. Även som fuktskydd på elektriska komponenter. |

Datum: 08-05-22 Ersätter: -

**Övriga uppgifter:** De tekniska uppgifterna bör betraktas som riktvärden.

Ingen tejp kan lagras under obegränsad tid. Livslängden för tejpen kan dock ökas genom att följa föreskrifterna. Lämpligt är att lagra tejperna i torr, mörk och sval lokal. Luftfuktighet ca 50 % och temperatur ca 15-20°C.

Då vi icke känner till de förhållanden under vilka tejperna lagras hos våra kunder, garanterar vi endast för tejpernas kvalitet vid leverans. Ansvar utöver fakturavärdet påtages ej.

EUROCOL TAPE AB

Eurocol Tape AB Box 117 SE-265 22 Åstorp Sweden T +46 (0) 42 – 668 00 F +46 (0) 42 – 668 05 www.eurocol.se info@eurocol.se

Bank SEB Åstorp 5652 1003089 Bankgiro 356-2535 Plusgiro 51 72 40-8 VAT No. SE556552383301

## *Table of figures*

## *Table of tables*